



Supplement of

Cold-water coral mounds are effective carbon sinks in the western Mediterranean Sea

Luis Greiffenhagen et al.

Correspondence to: Luis Greiffenhagen (lgreiffenhagen@marum.de)

The copyright of individual parts of the supplement might differ from the article licence.

Supplementary Material

S1 Calibration of GeoB18116-2 Dry Bulk Density (DBD) from CT scan data and pycnometer density measurements

CT analysis can be utilized reliably for sediment core density analyses (*sensu* Orsi *et al.*, 1994; Gerland and Villinger, 1995) with the advantage of much higher resolution, non-invasive sampling and substantial reduction of lab work. This is based on a general link between the density of an object and the attenuation of x-rays by the object (Orsi and Anderson, 1999; Duchesne *et al.*, 2009).

Upon comparing the Pycnometer-based classical density measurements of GeoB18116-2 with the 5 cm-average values from the CT on “Mean x-ray attenuation of matrix sediment [HU]”, a high correlation was found ($R^2 = 0.89$; $p\text{-val.} = < 0.0001$, Spearman’s test; normally distributed according to Shapiro-wilk test; no heteroscedasticity, Breusch-Pagan test $p = 0.45$). This regression-based validation method illustrates how CT data can be used as a proxy for DBD. Therefore, we here use our lab-measured pycnometer-based density samples throughout the record to calibrate the density profile of the entire core (see Orsi and Anderson, 1999). Assuming a linear regression equation of $Y = 868 * X + 205$, with DBD as independent variable, we calculated density X from CT mean x-ray attenuation Y (see Fig. 1).

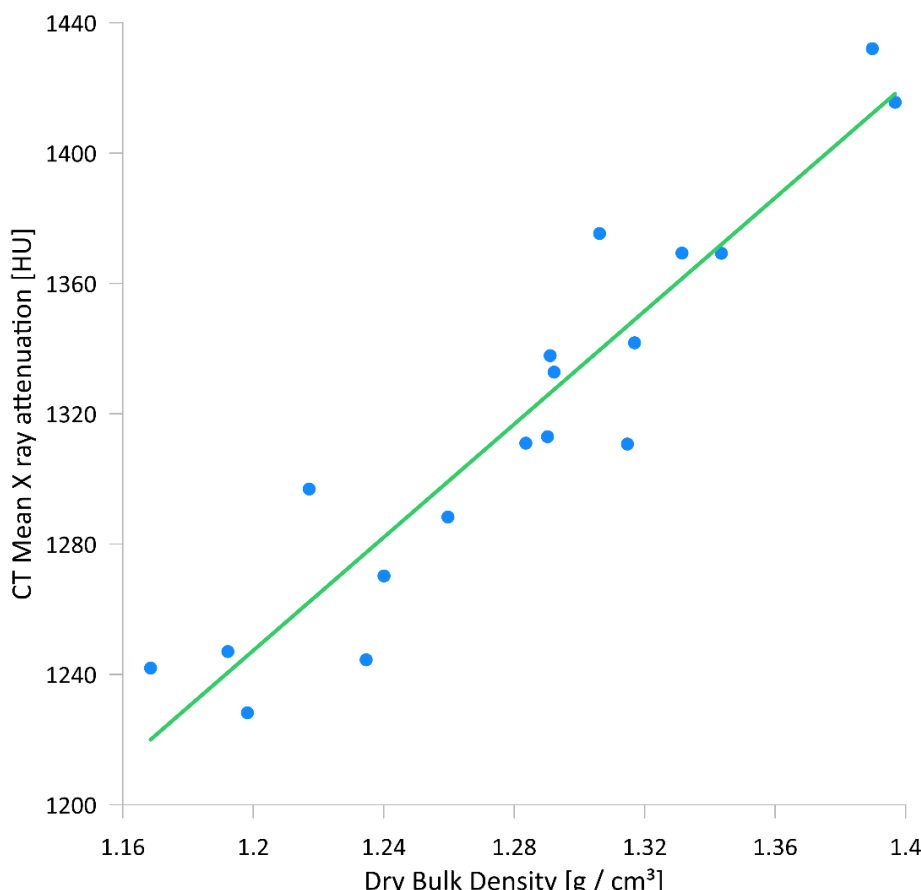


Fig. S1: Cross-Plot with linear regression fit, plotting Dry Bulk Density (measured with pycnometer) against mean X ray attenuation (CT derived high-resolution data). Regression function $Y = 868 * X + 205$.

S2 Raw Data of TIC/TOC and Density Measurements

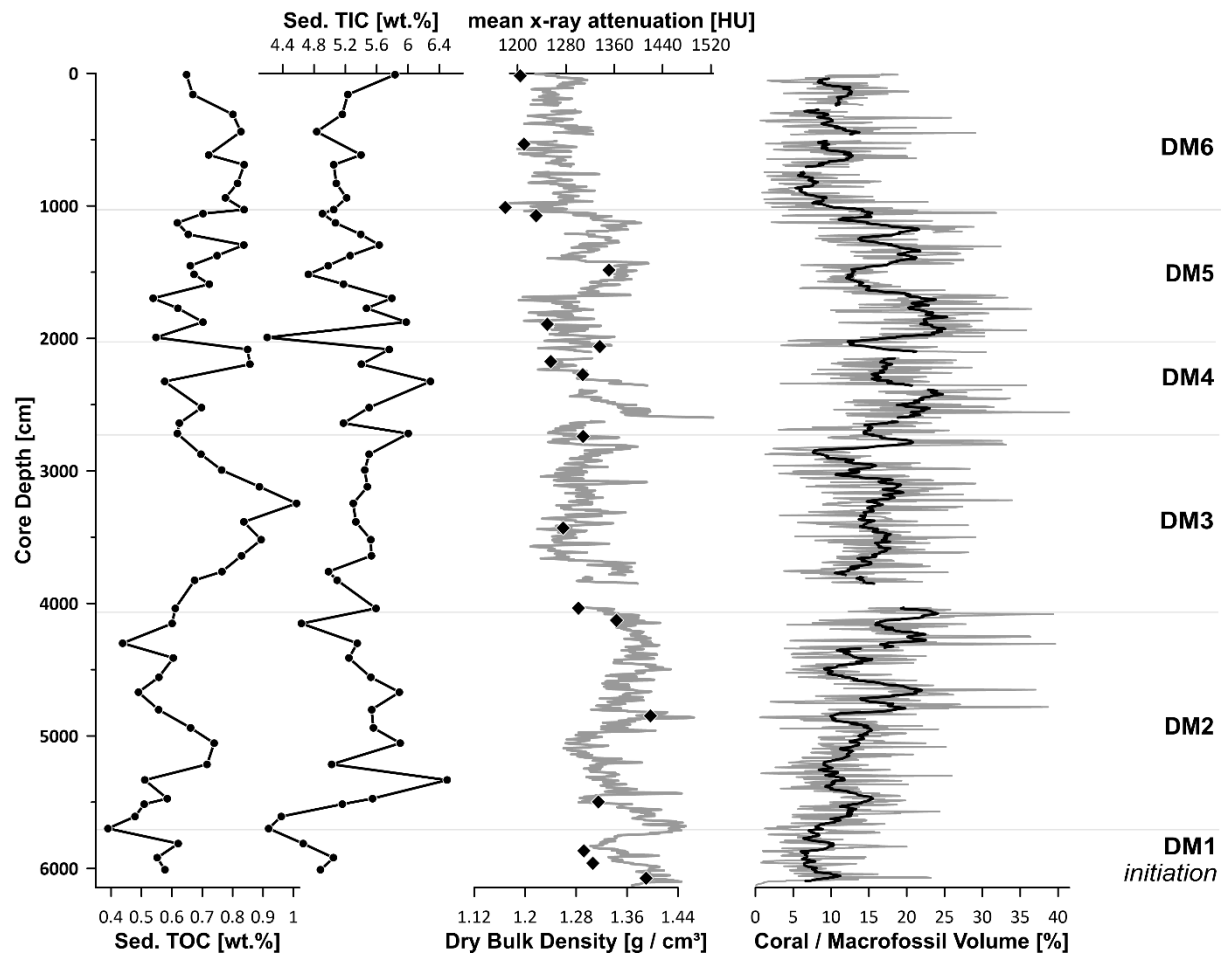


Fig. S2: Raw data summary from Dragon Mound (GeoB18116-2) measurements, based on new core depth model (CSF-B). TIC/TOC values ($n = 53$) are given in wt.% and refer to the sediment fraction of the record. Dry Bulk Density refers to black dashed line / points. Correlation between CT data and measured density data is clearly visible. Coral volume shows full 5 cm average (grey) and smoothed line (30 cm average) in black. CT / DBD data gaps are due to the recovery < 100 % in some MeBo barrel sections.

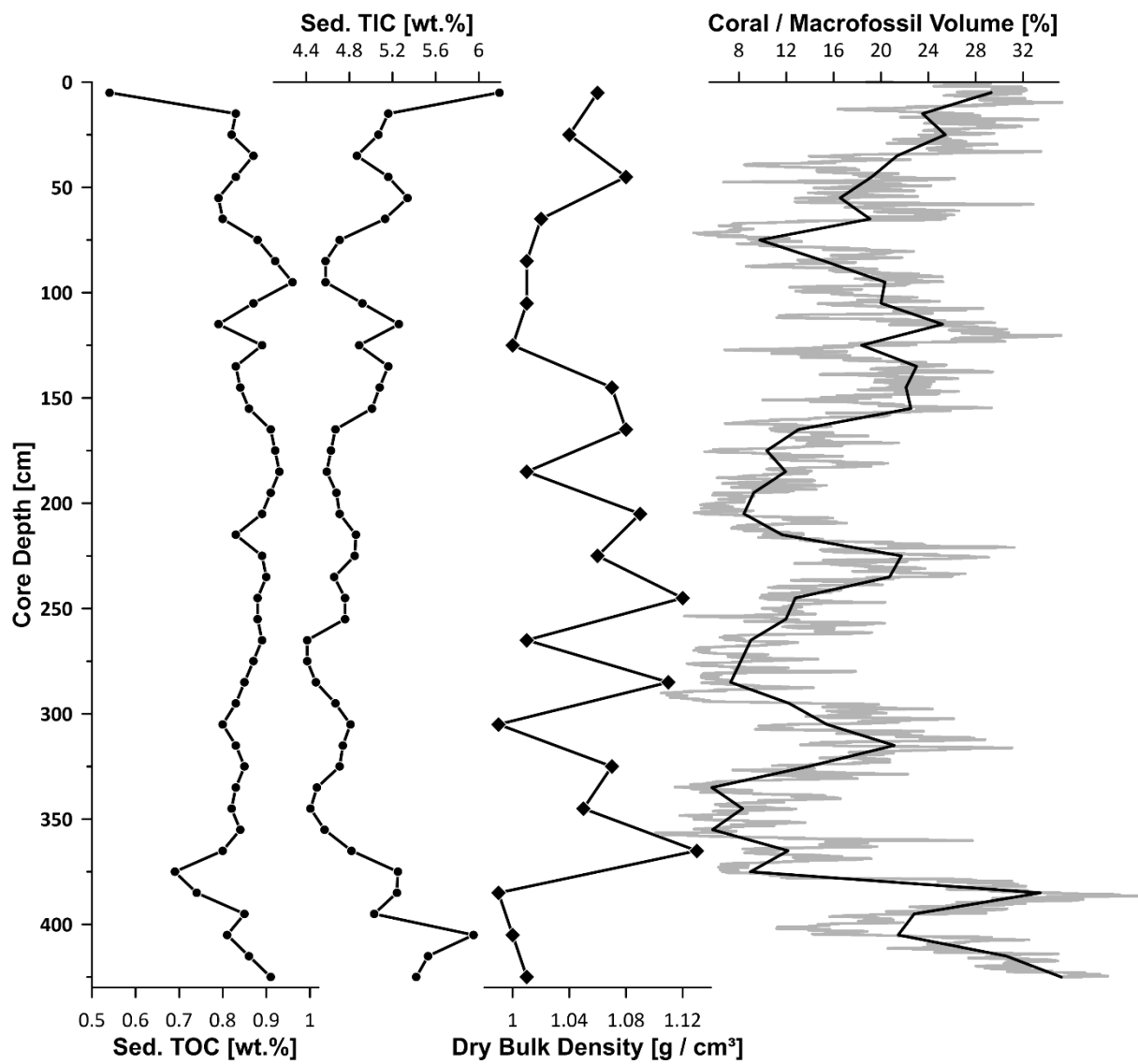


Fig. S3: Raw data summary from BRI (GeoB13729-1) measurements, based on published data. TIC/TOC values ($n = 44$; obtained by Wang et al., 2021) are given in wt.% and refer to the sediment fraction of the record. Dry Bulk Density ($n = 22$) is based on pycnometer measurements by Wang et al. (2021). CT coral content data (vol.%) are based on Titschack et al. (2016). Dark line shows smoothed 10 cm average, grey line represents the raw CT resolution.

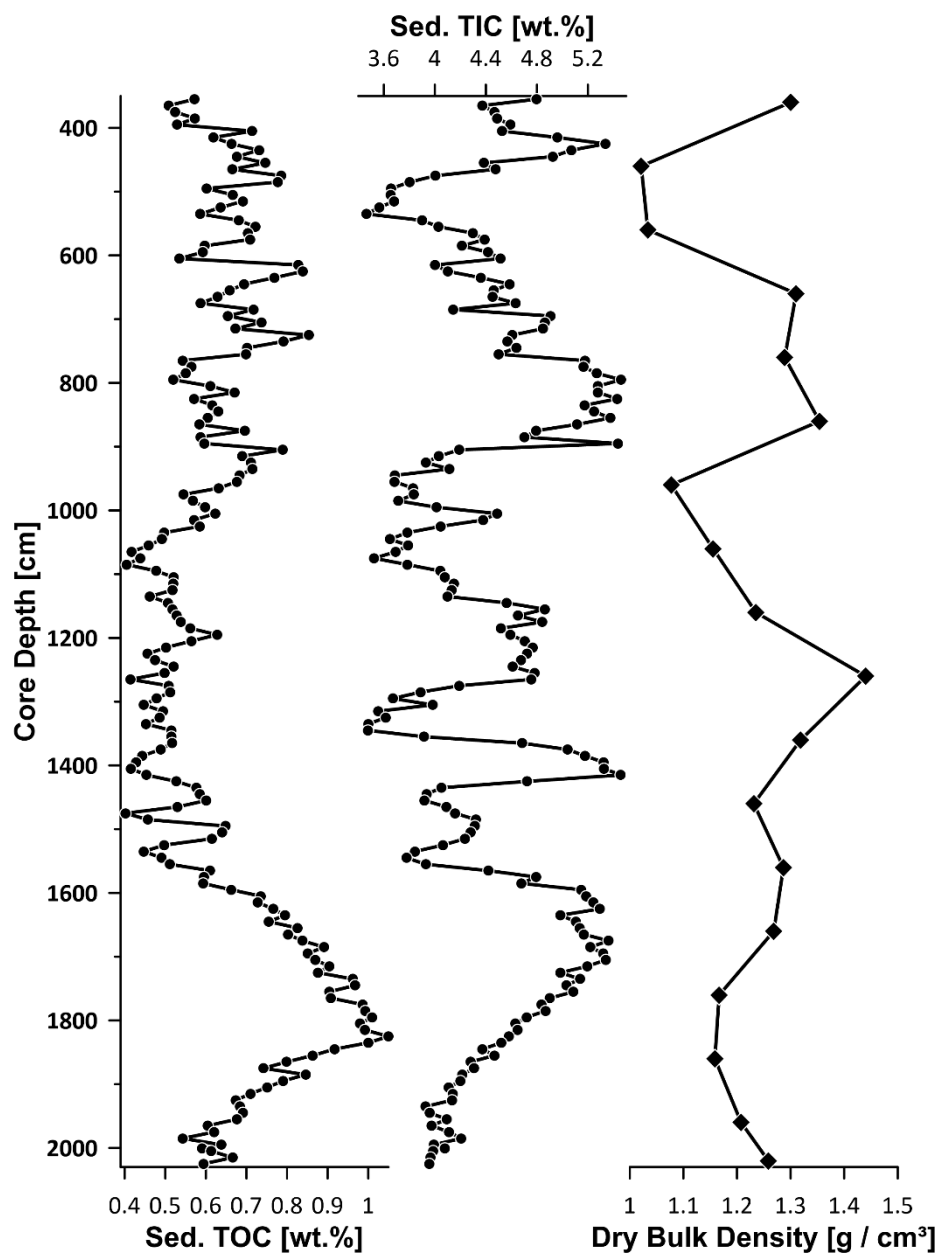
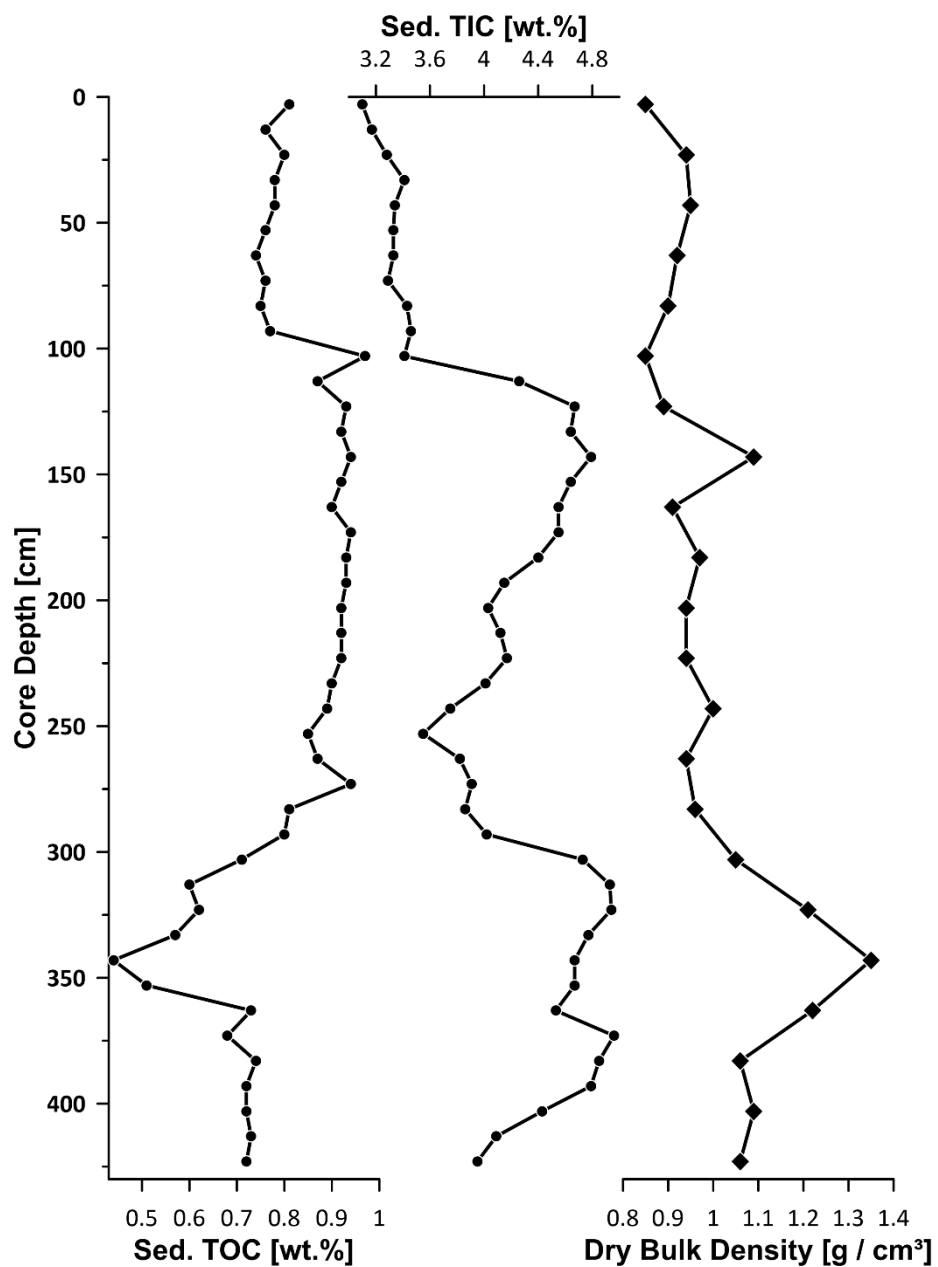


Fig. S4: Raw data summary from Off-Mound core MD13-3457 measurements. TIC/TOC values ($n = 169$) are given in wt.%. Dry Bulk Density is based on pycnometer measurements ($n = 21$), all conducted for this study.



S3 Sedimentation Rates, off mound cores

Undatable was used as a novel approach to create age models from marine fossils. However, a linear interpolation between the calibrated AMS ^{14}C ages was favoured over the 1 cm resolution sedimentation rates given in Undatable (based on Gaussian uncertainty sampling).

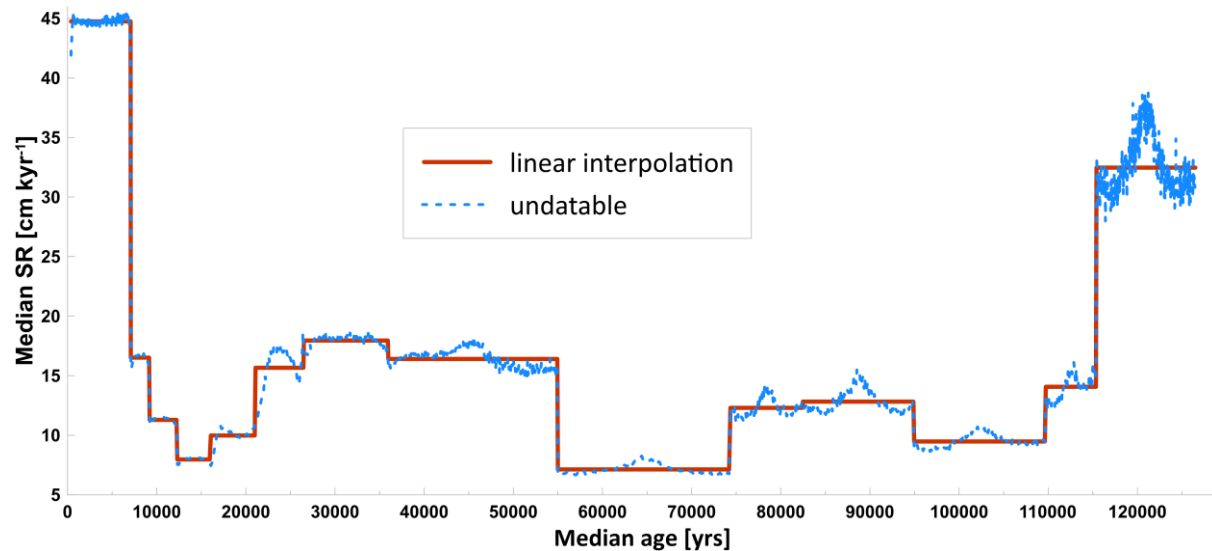


Fig. S6: Median AR (aggradation rate) of off-mound core MD13-3457 across time. Blue dotted line represents the initial age model from Undatable, while the red line represents the linear interpolation between the ages / tie points used in the study.

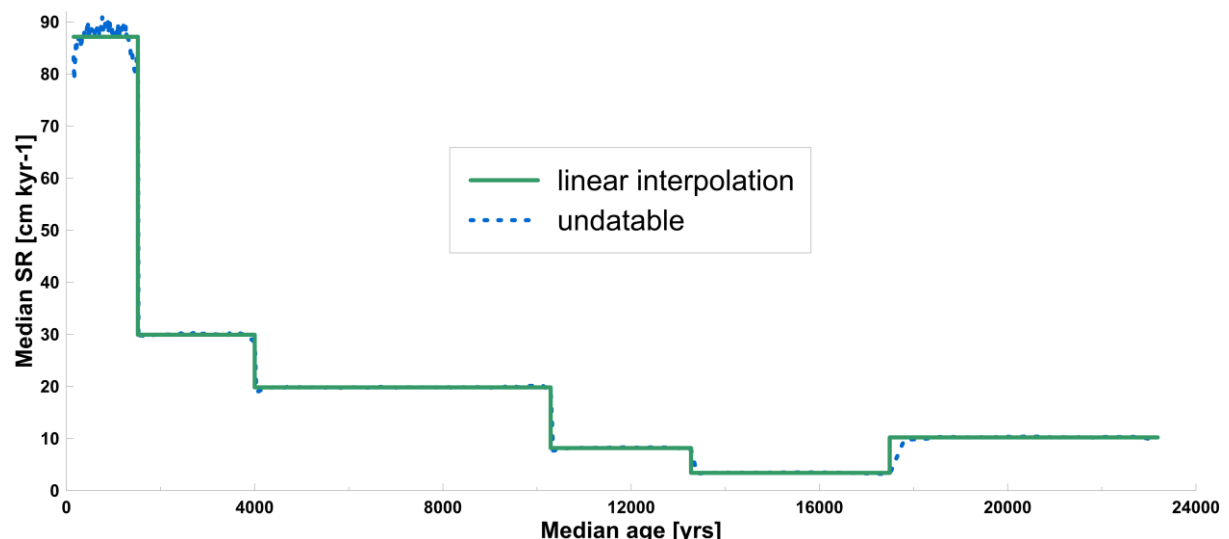


Fig. S7: Median AR (aggradation rate) of off-mound core GeoB13731-1 across time. Blue dotted line represents the initial age model from Undatable, while the green line represents the linear interpolation between the ages used in the study.

S4 AMS ^{14}C ages and tie points obtained for MD13-3457

Table S1: All ages used for this study from MD13-3457. Sample 1-8 are based on AMS ^{14}C dating, the others are tie points based on the $\delta^{18}\text{O}$ data from MD13-3457 and the global LR04 stack by Lisiecki and Raymo (2005).

Sample ID	Depth [m]	Raw Age [kyr BP]	Age error [kyr BP]	Dating Method	Reserv. Age [kyr BP]	Reserv. Error [kyr BP]	Calibration	Calib. Age [kyr BP]
1	0.03	0.75	0.03	^{14}C marine fossil	0.422	0.050	IntCal20	0.391
2	3.03	6.69	0.05	^{14}C marine fossil	0.483	0.051	IntCal20	7.095
3	3.38	8.59	0.05	^{14}C marine fossil	0.349	0.057	IntCal20	9.214
4	3.73	10.54	0.06	^{14}C marine fossil	0.108	0.052	IntCal20	12.314
5	4.03	13.47	0.08	^{14}C marine fossil	0.117	0.188	IntCal20	16.077
6	4.53	22.51	0.15	^{14}C marine fossil	0.157	0.268	IntCal20	21.087
7	5.38	22.37	0.40	^{14}C marine fossil	0.190	0.263	IntCal20	26.513
8	7.08	31.80	0.50	^{14}C marine fossil	0.178	0.219	IntCal20	35.982
s1	10.2	55.00	4.00	tie point	n/a	n/a	n/a	55.000
s2	11.58	75.00	4.00	tie point	n/a	n/a	n/a	74.351
s3	12.58	82.50	4.00	tie point	n/a	n/a	n/a	82.479
s4	14.18	95.00	4.00	tie point	n/a	n/a	n/a	94.955
s5	15.58	112.00	4.00	tie point	n/a	n/a	n/a	109.726
s6	16.38	115.50	4.00	tie point	n/a	n/a	n/a	115.412
s7	19.98	126.50	4.00	tie point	n/a	n/a	n/a	126.499

S5 $\delta^{18}\text{O}$ ‰ curve MD13-3457 and corresponding tie points for age model construction

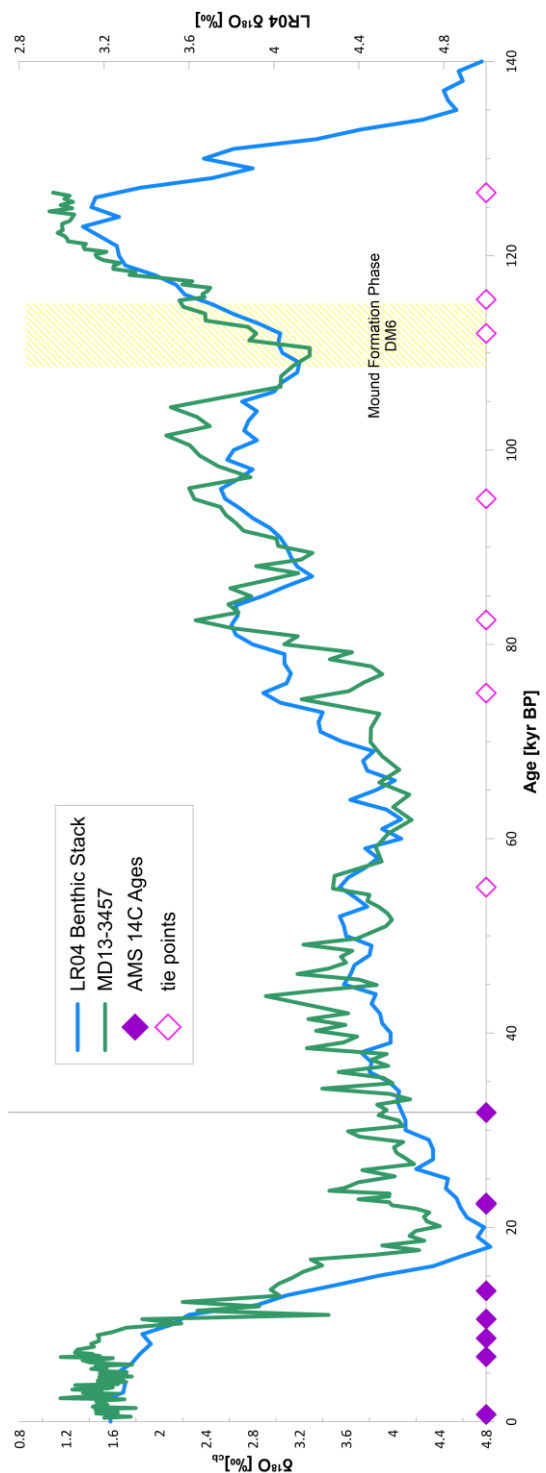


Fig. S8: Visual alignment of LR04 benthic stack and the $\delta^{18}\text{O}$ ‰ curve based on Stable oxygen isotopes ($\delta^{18}\text{O}$) obtained from the benthic foraminifera *Cibicidoides mundulus*. Dated ages and tie points are indicated. Yellow box indicated the period of mound formation during MIS5d on Dragon Mound (DM6).

S6 carbon accumulation rates off-mound during BRI_{final} and DM6

Table S2: Values from both off-mound records GeoB13731-1 and MD13-3457. Values identified as corresponding to the mound formation phases of BRI_{final} (9 – 12 kyr BP; MIS1) and DM6 (~108 – 115 kyr BP; MIS5) are separated by horizontal lines and in bold. Ages and sedimentation rates (SR) based on age models above. DBD for Dry Bulk Density. TOC/TIC values given in content weight-%. C(in)org Acc stands for (in)organic carbon accumulation. Note that mean values presented in the manuscript are based on weighted sedimentation rate means.

Core	Depth [cm]	Age [kyr BP]	TOC [%]	TIC [%]	DBD [g/cm ³]	SR [cm kyr ⁻¹]	C _{org} Acc [g cm ⁻² ky ⁻¹]	C _{inorg} Acc [g cm ⁻² ky ⁻¹]	Total Carbon Acc [g cm ⁻² ky ⁻¹]
GeoB13731-1	13	0.22	0.76	3.17	0.90	87.15	0.59	2.47	3.07
GeoB13731-1	23	0.33	0.8	3.28	0.94	87.15	0.66	2.69	3.34
GeoB13731-1	33	0.45	0.78	3.41	0.95	87.15	0.64	2.81	3.45
GeoB13731-1	43	0.56	0.78	3.34	0.95	87.15	0.65	2.77	3.41
GeoB13731-1	53	0.67	0.76	3.33	0.94	87.15	0.62	2.71	3.33
GeoB13731-1	63	0.78	0.74	3.33	0.92	87.15	0.59	2.67	3.26
GeoB13731-1	73	0.90	0.76	3.29	0.91	87.15	0.60	2.61	3.21
GeoB13731-1	83	1.01	0.75	3.43	0.90	87.15	0.59	2.69	3.28
GeoB13731-1	93	1.12	0.77	3.46	0.88	87.15	0.59	2.64	3.23
GeoB13731-1	103	1.24	0.97	3.41	0.85	87.15	0.72	2.53	3.24
GeoB13731-1	113	1.35	0.87	4.26	0.87	87.15	0.66	3.23	3.89
GeoB13731-1	123	1.47	0.93	4.67	0.89	87.15	0.72	3.62	4.34
GeoB13731-1	133	1.70	0.92	4.64	0.99	29.93	0.27	1.37	1.65
GeoB13731-1	143	2.04	0.94	4.79	1.09	29.93	0.31	1.56	1.87
GeoB13731-1	153	2.37	0.92	4.64	1.00	29.93	0.28	1.39	1.66
GeoB13731-1	163	2.70	0.9	4.55	0.91	29.93	0.25	1.24	1.48
GeoB13731-1	173	3.03	0.94	4.55	0.94	29.93	0.26	1.28	1.54
GeoB13731-1	183	3.37	0.93	4.4	0.97	29.93	0.27	1.28	1.55
GeoB13731-1	193	3.70	0.93	4.15	0.96	29.93	0.27	1.19	1.45
GeoB13731-1	203	4.04	0.92	4.03	0.94	19.83	0.17	0.75	0.92
GeoB13731-1	213	4.55	0.92	4.12	0.94	19.83	0.17	0.77	0.94
GeoB13731-1	223	5.05	0.92	4.17	0.94	19.83	0.17	0.78	0.95
GeoB13731-1	233	5.56	0.9	4.01	0.97	19.83	0.17	0.77	0.94
GeoB13731-1	243	6.06	0.89	3.75	0.94	19.83	0.17	0.70	0.86
GeoB13731-1	253	6.57	0.85	3.55	0.91	19.83	0.15	0.64	0.79
GeoB13731-1	263	7.07	0.87	3.82	0.94	19.83	0.16	0.71	0.87
GeoB13731-1	273	7.57	0.94	3.91	0.95	19.83	0.18	0.74	0.91
GeoB13731-1	283	8.08	0.81	3.86	0.96	19.83	0.15	0.73	0.89
GeoB13731-1	293	8.58	0.8	4.02	1.01	19.8	0.16	0.8	0.96
GeoB13731-1	303	9.09	0.71	4.73	1.05	19.8	0.15	0.98	1.13
GeoB13731-1	313	9.59	0.6	4.93	1.13	19.8	0.13	1.1	1.24
GeoB13731-1	323	10.09	0.62	4.94	1.21	19.8	0.15	1.19	1.33
GeoB13731-1	333	10.97	0.57	4.77	1.28	8.2	0.06	0.5	0.56
GeoB13731-1	343	12.18	0.44	4.67	1.35	8.2	0.05	0.52	0.56
MD13-3457	375	12.58	0.52	4.47	1.26	7.97	0.05	0.45	0.50

MD13-3457	385	13.83	0.57	4.49	1.23	7.97	0.06	0.44	0.50
MD13-3457	395	15.06	0.53	4.59	1.20	7.97	0.05	0.44	0.49
MD13-3457	405	16.34	0.71	4.53	1.17	9.98	0.08	0.53	0.61
MD13-3457	415	17.36	0.62	4.96	1.15	9.98	0.07	0.57	0.64
MD13-3457	425	18.32	0.66	5.34	1.12	9.98	0.07	0.60	0.67
MD13-3457	435	19.32	0.73	5.07	1.09	9.98	0.08	0.55	0.63
MD13-3457	445	20.32	0.68	4.92	1.06	9.98	0.07	0.52	0.59
MD13-3457	455	21.27	0.75	4.38	1.04	15.67	0.12	0.71	0.83
MD13-3457	465	22.07	0.67	4.48	1.02	15.67	0.11	0.72	0.82
MD13-3457	475	22.71	0.79	4.00	1.02	15.67	0.13	0.64	0.77
MD13-3457	485	23.30	0.78	3.80	1.02	15.67	0.12	0.61	0.73
MD13-3457	495	23.88	0.60	3.66	1.03	15.67	0.10	0.59	0.68
MD13-3457	505	24.46	0.67	3.65	1.03	15.67	0.11	0.59	0.69
MD13-3457	515	25.06	0.69	3.68	1.03	15.67	0.11	0.59	0.70
MD13-3457	525	25.69	0.64	3.56	1.03	15.67	0.10	0.57	0.68
MD13-3457	535	26.35	0.59	3.46	1.03	15.67	0.09	0.56	0.65
MD13-3457	545	26.93	0.68	3.90	1.03	17.95	0.13	0.72	0.85
MD13-3457	555	27.51	0.72	4.03	1.03	17.95	0.13	0.75	0.88
MD13-3457	565	28.06	0.70	4.30	1.05	17.95	0.13	0.81	0.94
MD13-3457	575	28.61	0.71	4.39	1.08	17.95	0.14	0.85	0.98
MD13-3457	585	29.17	0.60	4.21	1.10	17.95	0.12	0.83	0.95
MD13-3457	595	29.72	0.59	4.42	1.13	17.95	0.12	0.90	1.02
MD13-3457	605	30.27	0.54	4.52	1.16	17.95	0.11	0.94	1.05
MD13-3457	615	30.82	0.83	4.00	1.19	17.95	0.18	0.85	1.03
MD13-3457	625	31.37	0.84	4.10	1.21	17.95	0.18	0.89	1.08
MD13-3457	635	31.91	0.77	4.36	1.24	17.95	0.17	0.97	1.14
MD13-3457	645	32.46	0.69	4.59	1.27	17.95	0.16	1.04	1.20
MD13-3457	655	33.01	0.66	4.46	1.30	17.95	0.15	1.04	1.19
MD13-3457	665	33.56	0.63	4.45	1.31	17.95	0.15	1.05	1.19
MD13-3457	675	34.11	0.59	4.63	1.31	17.95	0.14	1.09	1.23
MD13-3457	685	34.67	0.72	4.14	1.31	17.95	0.17	0.97	1.14
MD13-3457	695	35.23	0.65	4.91	1.30	17.95	0.15	1.15	1.30
MD13-3457	705	35.81	0.74	4.86	1.30	17.95	0.17	1.14	1.31
MD13-3457	715	36.43	0.67	4.85	1.30	16.41	0.14	1.03	1.18
MD13-3457	725	37.05	0.85	4.61	1.30	16.41	0.18	0.98	1.16
MD13-3457	735	37.66	0.79	4.57	1.29	16.41	0.17	0.97	1.14
MD13-3457	745	38.26	0.70	4.64	1.29	16.41	0.15	0.98	1.13
MD13-3457	755	38.86	0.70	4.50	1.29	16.41	0.15	0.95	1.10
MD13-3457	765	39.45	0.54	5.18	1.29	16.41	0.12	1.10	1.21
MD13-3457	775	40.05	0.56	5.17	1.30	16.41	0.12	1.10	1.22
MD13-3457	785	40.65	0.55	5.27	1.31	16.41	0.12	1.13	1.25
MD13-3457	795	41.25	0.52	5.46	1.31	16.41	0.11	1.18	1.29
MD13-3457	805	41.85	0.61	5.28	1.32	16.41	0.13	1.14	1.27
MD13-3457	815	42.44	0.67	5.28	1.32	16.41	0.15	1.15	1.29
MD13-3457	825	43.04	0.57	5.43	1.33	16.41	0.12	1.19	1.31
MD13-3457	835	43.62	0.62	5.17	1.34	16.41	0.14	1.14	1.27
MD13-3457	845	44.20	0.63	5.25	1.34	16.41	0.14	1.16	1.30

MD13-3457	855	44.77	0.61	5.38	1.35	16.41	0.13	1.19	1.33
MD13-3457	865	45.34	0.58	5.12	1.34	16.41	0.13	1.12	1.25
MD13-3457	875	45.90	0.70	4.79	1.31	16.41	0.15	1.03	1.18
MD13-3457	885	46.47	0.59	4.70	1.28	16.41	0.12	0.99	1.11
MD13-3457	895	47.06	0.60	5.43	1.26	16.41	0.12	1.12	1.24
MD13-3457	905	47.66	0.79	4.19	1.23	16.41	0.16	0.85	1.00
MD13-3457	915	48.28	0.69	4.03	1.20	16.41	0.14	0.79	0.93
MD13-3457	925	48.91	0.71	3.93	1.17	16.41	0.14	0.76	0.89
MD13-3457	935	49.53	0.72	4.12	1.15	16.41	0.13	0.77	0.91
MD13-3457	945	50.17	0.68	3.69	1.12	16.41	0.13	0.68	0.80
MD13-3457	955	50.81	0.68	3.68	1.09	16.41	0.12	0.66	0.78
MD13-3457	965	51.46	0.63	3.83	1.08	16.41	0.11	0.68	0.79
MD13-3457	975	52.11	0.55	3.84	1.09	16.41	0.10	0.69	0.78
MD13-3457	985	52.75	0.57	3.71	1.10	16.41	0.10	0.67	0.77
MD13-3457	995	53.40	0.60	4.01	1.10	16.41	0.11	0.73	0.84
MD13-3457	1005	54.04	0.62	4.49	1.11	16.41	0.11	0.82	0.93
MD13-3457	1015	54.68	0.57	4.38	1.12	16.41	0.10	0.80	0.91
MD13-3457	1025	55.73	0.59	4.05	1.13	7.13	0.05	0.33	0.37
MD13-3457	1035	57.21	0.50	3.78	1.14	7.13	0.04	0.31	0.35
MD13-3457	1045	58.68	0.49	3.65	1.14	7.13	0.04	0.30	0.34
MD13-3457	1055	60.12	0.46	3.79	1.15	7.13	0.04	0.31	0.35
MD13-3457	1065	61.52	0.42	3.69	1.16	7.13	0.03	0.31	0.34
MD13-3457	1075	62.88	0.44	3.52	1.17	7.13	0.04	0.29	0.33
MD13-3457	1085	64.16	0.41	3.79	1.18	7.13	0.03	0.32	0.35
MD13-3457	1095	65.41	0.48	4.04	1.18	7.13	0.04	0.34	0.38
MD13-3457	1105	66.70	0.52	4.08	1.19	7.13	0.04	0.35	0.39
MD13-3457	1115	68.07	0.52	4.15	1.20	7.13	0.04	0.35	0.40
MD13-3457	1125	69.49	0.52	4.13	1.21	7.13	0.04	0.36	0.40
MD13-3457	1135	70.95	0.46	4.10	1.22	7.13	0.04	0.36	0.40
MD13-3457	1145	72.42	0.51	4.56	1.22	7.13	0.04	0.40	0.44
MD13-3457	1155	73.91	0.52	4.86	1.23	7.13	0.05	0.43	0.47
MD13-3457	1165	74.94	0.53	4.65	1.25	12.30	0.08	0.71	0.79
MD13-3457	1175	75.81	0.54	4.84	1.27	12.30	0.08	0.75	0.84
MD13-3457	1185	76.67	0.56	4.52	1.29	12.30	0.09	0.72	0.80
MD13-3457	1195	77.50	0.63	4.59	1.31	12.30	0.10	0.74	0.84
MD13-3457	1205	78.25	0.56	4.71	1.33	12.30	0.09	0.77	0.86
MD13-3457	1215	78.97	0.50	4.77	1.35	12.30	0.08	0.79	0.87
MD13-3457	1225	79.75	0.46	4.72	1.37	12.30	0.08	0.80	0.87
MD13-3457	1235	80.58	0.48	4.68	1.39	12.30	0.08	0.80	0.88
MD13-3457	1245	81.43	0.52	4.61	1.41	12.30	0.09	0.80	0.89
MD13-3457	1255	82.24	0.50	4.78	1.43	12.30	0.09	0.84	0.93
MD13-3457	1265	83.05	0.41	4.76	1.43	12.82	0.08	0.87	0.95
MD13-3457	1275	83.87	0.51	4.19	1.42	12.82	0.09	0.76	0.86
MD13-3457	1285	84.70	0.51	3.89	1.41	12.82	0.09	0.70	0.80
MD13-3457	1295	85.53	0.48	3.67	1.40	12.82	0.09	0.66	0.74
MD13-3457	1305	86.33	0.45	3.98	1.39	12.82	0.08	0.71	0.79
MD13-3457	1315	87.10	0.49	3.56	1.37	12.82	0.09	0.63	0.71

MD13-3457	1325	87.84	0.49	3.61	1.36	12.82	0.08	0.63	0.72
MD13-3457	1335	88.53	0.45	3.48	1.35	12.82	0.08	0.60	0.68
MD13-3457	1345	89.21	0.52	3.48	1.34	12.82	0.09	0.60	0.68
MD13-3457	1355	89.91	0.52	3.92	1.32	12.82	0.09	0.67	0.75
MD13-3457	1365	90.66	0.52	4.68	1.31	12.82	0.09	0.79	0.88
MD13-3457	1375	91.45	0.49	5.04	1.31	12.82	0.08	0.84	0.93
MD13-3457	1385	92.25	0.44	5.18	1.30	12.82	0.07	0.86	0.93
MD13-3457	1395	93.07	0.43	5.32	1.29	12.82	0.07	0.88	0.95
MD13-3457	1405	93.90	0.42	5.33	1.28	12.82	0.07	0.87	0.94
MD13-3457	1415	94.71	0.45	5.46	1.27	12.82	0.07	0.89	0.96
MD13-3457	1425	95.74	0.53	4.72	1.26	9.48	0.06	0.56	0.63
MD13-3457	1435	96.86	0.58	4.05	1.25	9.48	0.07	0.48	0.55
MD13-3457	1445	97.99	0.59	3.94	1.24	9.48	0.07	0.46	0.53
MD13-3457	1455	99.11	0.60	3.92	1.24	9.48	0.07	0.46	0.53
MD13-3457	1465	100.18	0.53	4.09	1.23	9.48	0.06	0.48	0.54
MD13-3457	1475	101.20	0.40	4.16	1.24	9.48	0.05	0.49	0.54
MD13-3457	1485	102.17	0.46	4.32	1.25	9.48	0.05	0.51	0.56
MD13-3457	1495	103.13	0.65	4.31	1.25	9.48	0.08	0.51	0.59
MD13-3457	1505	104.10	0.64	4.28	1.26	9.48	0.08	0.51	0.59
MD13-3457	1515	105.13	0.62	4.24	1.26	9.48	0.07	0.51	0.58
MD13-3457	1525	106.19	0.50	4.06	1.27	9.48	0.06	0.49	0.55
MD13-3457	1535	107.27	0.45	3.84	1.27	9.48	0.05	0.46	0.52
MD13-3457	1545	108.34	0.49	3.78	1.28	9.48	0.06	0.46	0.52
MD13-3457	1555	109.41	0.51	3.93	1.28	9.48	0.06	0.48	0.54
MD13-3457	1565	110.27	0.61	4.42	1.29	14.07	0.11	0.80	0.91
MD13-3457	1575	111.05	0.60	4.80	1.28	14.07	0.11	0.87	0.97
MD13-3457	1585	111.80	0.59	4.68	1.28	14.07	0.11	0.84	0.95
MD13-3457	1595	112.48	0.66	5.15	1.28	14.07	0.12	0.93	1.05
MD13-3457	1605	113.13	0.74	5.19	1.28	14.07	0.13	0.93	1.06
MD13-3457	1615	113.83	0.73	5.24	1.28	14.07	0.13	0.94	1.07
MD13-3457	1625	114.54	0.77	5.29	1.27	14.07	0.14	0.95	1.09
MD13-3457	1635	115.21	0.80	4.99	1.27	14.07	0.14	0.89	1.04
MD13-3457	1645	115.64	0.76	5.11	1.27	32.47	0.31	2.11	2.42
MD13-3457	1655	115.96	0.83	5.13	1.27	32.47	0.34	2.12	2.46
MD13-3457	1665	116.28	0.80	5.17	1.26	32.47	0.33	2.12	2.45
MD13-3457	1675	116.61	0.84	5.36	1.25	32.47	0.34	2.18	2.52
MD13-3457	1685	116.94	0.89	5.22	1.24	32.47	0.36	2.11	2.47
MD13-3457	1695	117.27	0.85	5.32	1.23	32.47	0.34	2.13	2.47
MD13-3457	1705	117.60	0.87	5.34	1.22	32.47	0.35	2.12	2.47
MD13-3457	1715	117.92	0.90	5.20	1.21	32.47	0.36	2.05	2.40
MD13-3457	1725	118.24	0.88	4.98	1.20	32.47	0.34	1.95	2.29
MD13-3457	1735	118.55	0.96	5.14	1.19	32.47	0.37	1.99	2.36
MD13-3457	1745	118.86	0.97	5.03	1.18	32.47	0.37	1.93	2.30
MD13-3457	1755	119.17	0.90	5.09	1.17	32.47	0.34	1.94	2.28
MD13-3457	1765	119.46	0.91	4.90	1.17	32.47	0.34	1.86	2.20
MD13-3457	1775	119.75	0.99	4.83	1.17	32.47	0.37	1.83	2.20
MD13-3457	1785	120.04	0.99	4.87	1.16	32.47	0.38	1.84	2.22

MD13-3457	1795	120.33	1.01	4.72	1.16	32.47	0.38	1.78	2.17
MD13-3457	1805	120.60	0.98	4.63	1.16	32.47	0.37	1.75	2.12
MD13-3457	1815	120.87	0.99	4.65	1.16	32.47	0.37	1.75	2.13
MD13-3457	1825	121.14	1.05	4.58	1.16	32.47	0.40	1.73	2.12
MD13-3457	1835	121.41	1.00	4.52	1.16	32.47	0.38	1.70	2.08
MD13-3457	1845	121.68	0.92	4.37	1.16	32.47	0.35	1.65	1.99
MD13-3457	1855	121.97	0.86	4.47	1.16	32.47	0.32	1.68	2.01
MD13-3457	1865	122.26	0.80	4.28	1.16	32.47	0.30	1.61	1.92
MD13-3457	1875	122.56	0.74	4.31	1.17	32.47	0.28	1.63	1.91
MD13-3457	1885	122.87	0.85	4.21	1.17	32.47	0.32	1.60	1.92
MD13-3457	1895	123.19	0.79	4.20	1.18	32.47	0.30	1.60	1.91
MD13-3457	1905	123.50	0.75	4.11	1.18	32.47	0.29	1.58	1.86
MD13-3457	1915	123.82	0.71	4.14	1.19	32.47	0.27	1.59	1.87
MD13-3457	1925	124.15	0.67	4.14	1.19	32.47	0.26	1.60	1.86
MD13-3457	1935	124.47	0.68	3.93	1.20	32.47	0.27	1.52	1.79
MD13-3457	1945	124.80	0.69	3.96	1.20	32.47	0.27	1.54	1.81
MD13-3457	1955	125.12	0.68	4.09	1.21	32.47	0.26	1.60	1.87
MD13-3457	1965	125.44	0.61	3.98	1.21	32.47	0.24	1.56	1.80
MD13-3457	1975	125.76	0.62	4.11	1.22	32.47	0.25	1.63	1.87
MD13-3457	1985	126.08	0.54	4.21	1.23	32.47	0.22	1.68	1.90
MD13-3457	1995	126.40	0.64	3.99	1.24	32.47	0.26	1.60	1.86

S7 CT scans of Dragon Mound (GeoB18116-2)

The following section provides all obtained CT data in this study, referring to the 60 m long CT scan of Dragon Mound, consisting of 26 barrels. Each figure shows, from left to right, CT orthoslice, 3D macrofossil reconstruction, a mean grain size distribution plot as well as a clast orientation plot, several graphs representing coral content (vol. %), the mean x-ray attenuation in Hounsfield Units [HU], and its standard deviation, all along the corresponding core depth. To avoid distortion of the CT images, the following figures show the core depth based on CSF-A.

GeoB18116-2 P1

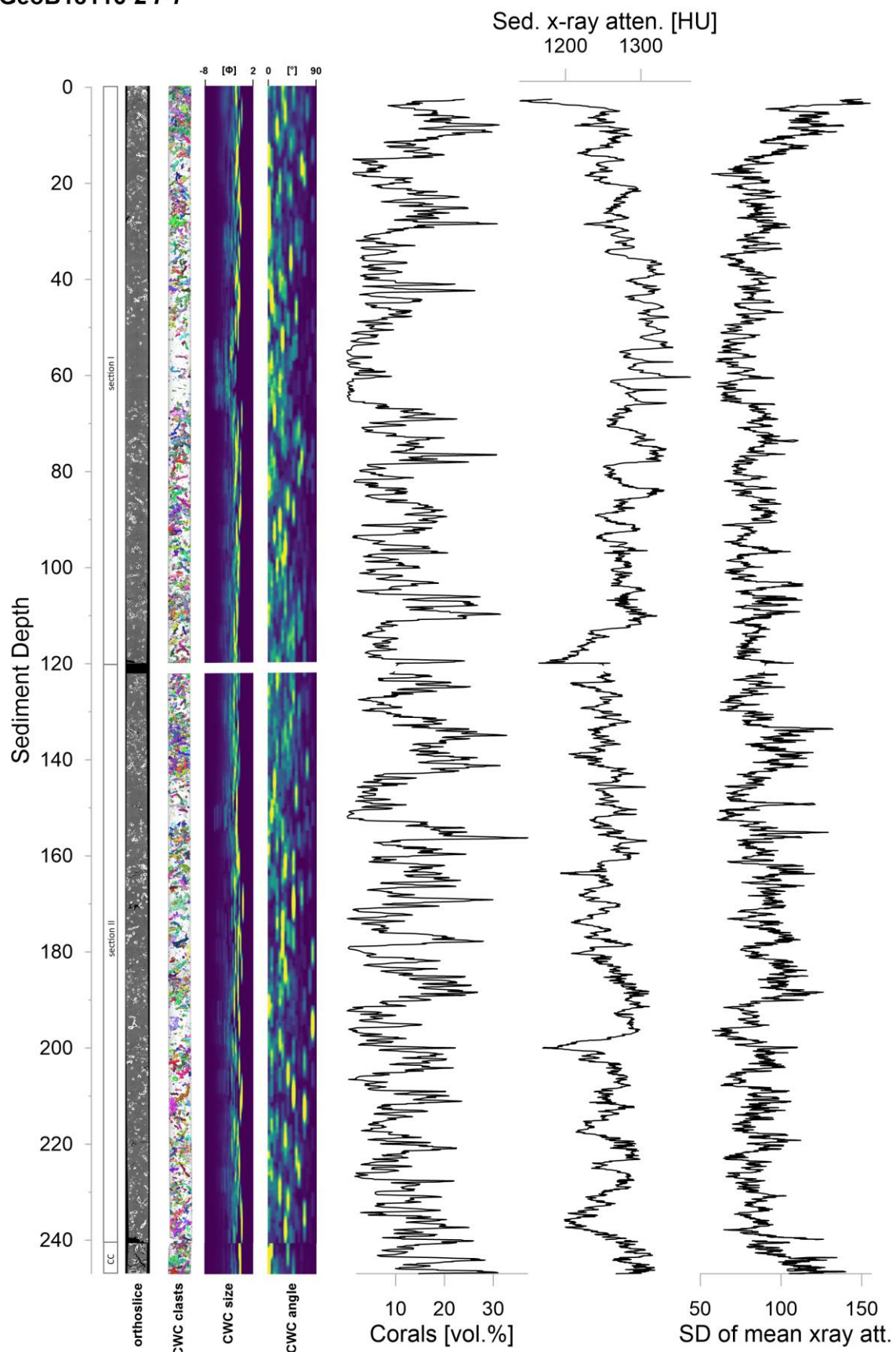


Fig. S9: CT-derived core data for GeoB18116-2 Barrel P1, with Sediment Depth as CSF-A (mbsf), orthoslice, section number (CC = core catcher), cold-water coral fossil clast quantification, size and angle, coral volume and mean x-ray attenuation in HU (Hounsfield units), and SD.

GeoB18116-2 P2

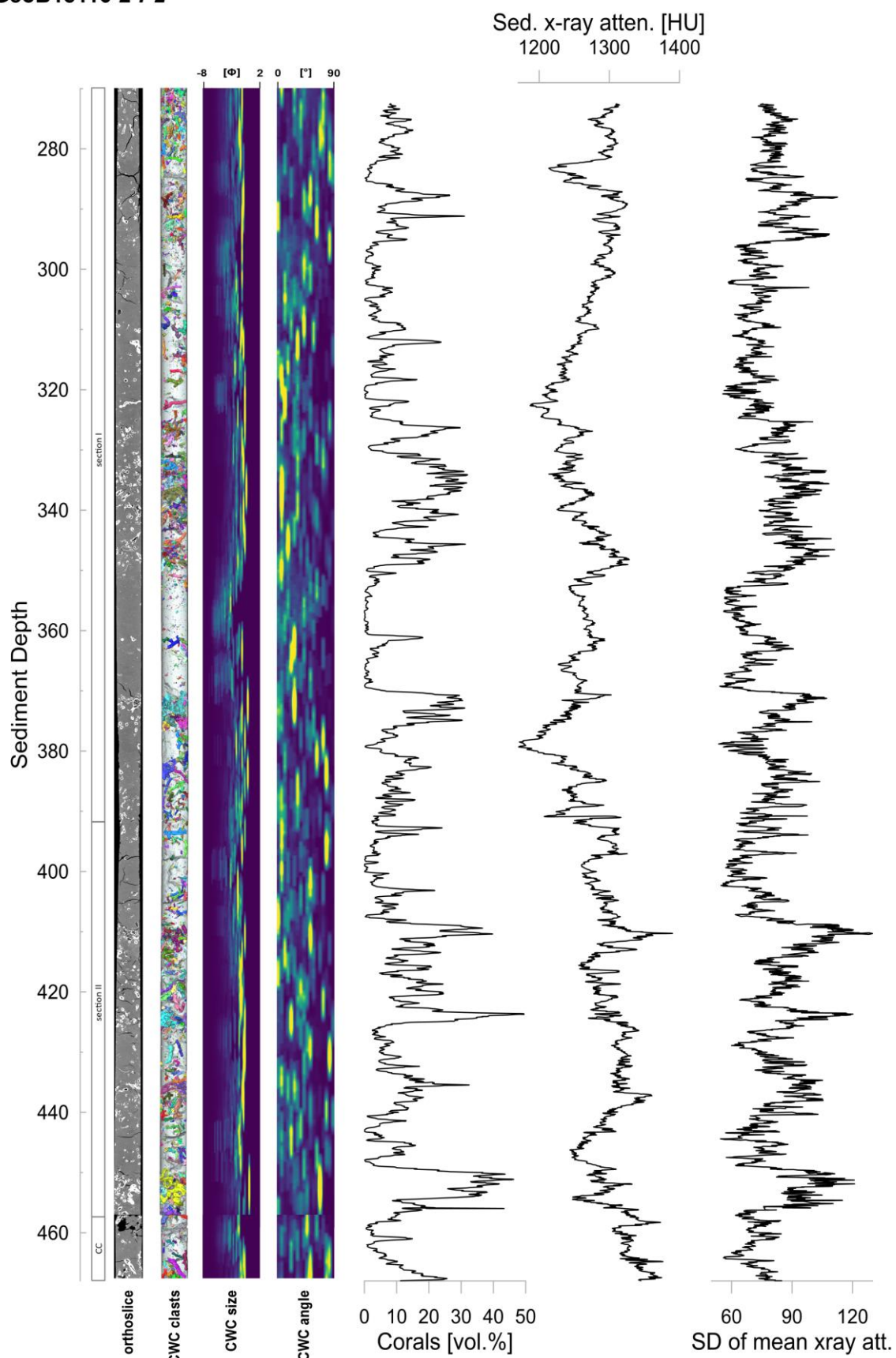


Fig. S10: CT-derived core data for GeoB18116-2 Barrel P2, with Sediment Depth as CSF-A (mbsf), orthoslice, section number (CC = core catcher), cold-water coral fossil clast quantification, size and angle, coral volume and mean x-ray attenuation in HU (Hounsfield units), and SD.

GeoB18116-2 P3

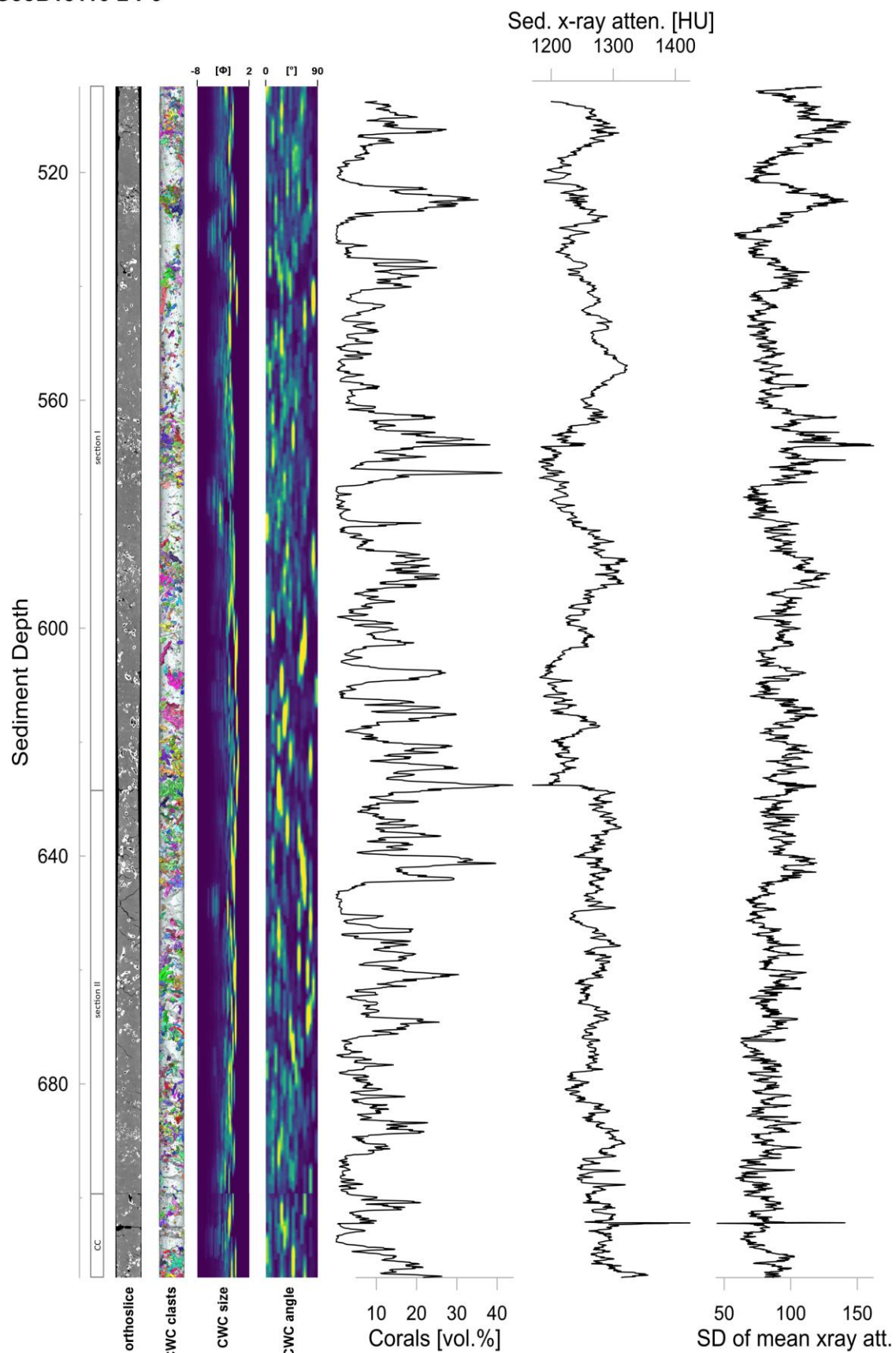


Fig. S11: CT-derived core data for GeoB18116-2 Barrel P3, with Sediment Depth as CSF-A (mbsf), orthoslice, section number (CC = core catcher), cold-water coral fossil clast quantification, size and angle, coral volume and mean x-ray attenuation in HU (Hounsfield units), and SD.

GeoB18116-2 P4

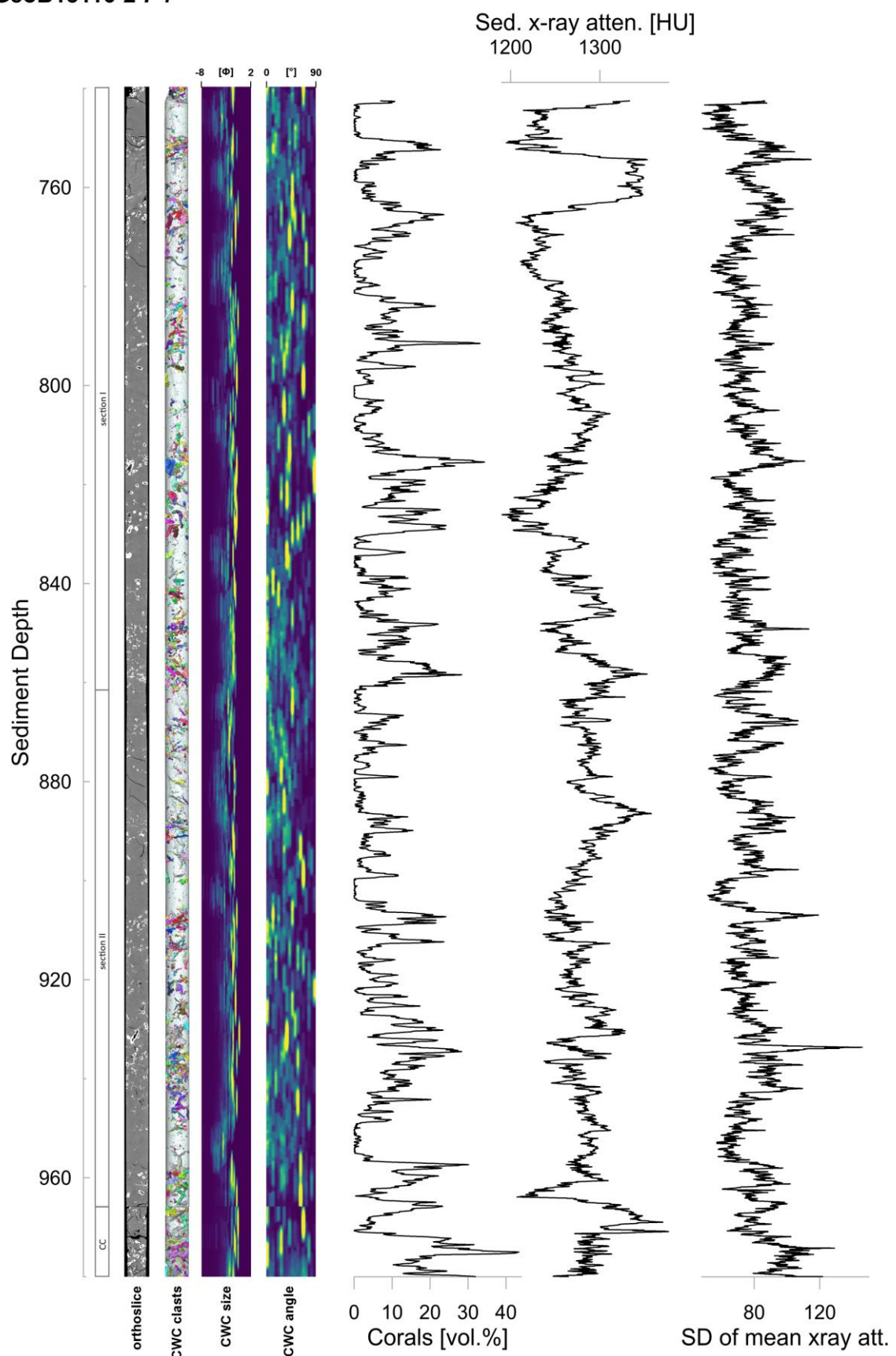


Fig. S12: CT-derived core data for GeoB18116-2 Barrel P4, with Sediment Depth as CSF-A (mbsf), orthoslice, section number (CC = core catcher), cold-water coral fossil clast quantification, size and angle, coral volume and mean x-ray attenuation in HU (Hounsfield units), and SD.

GeoB18116-2 P5

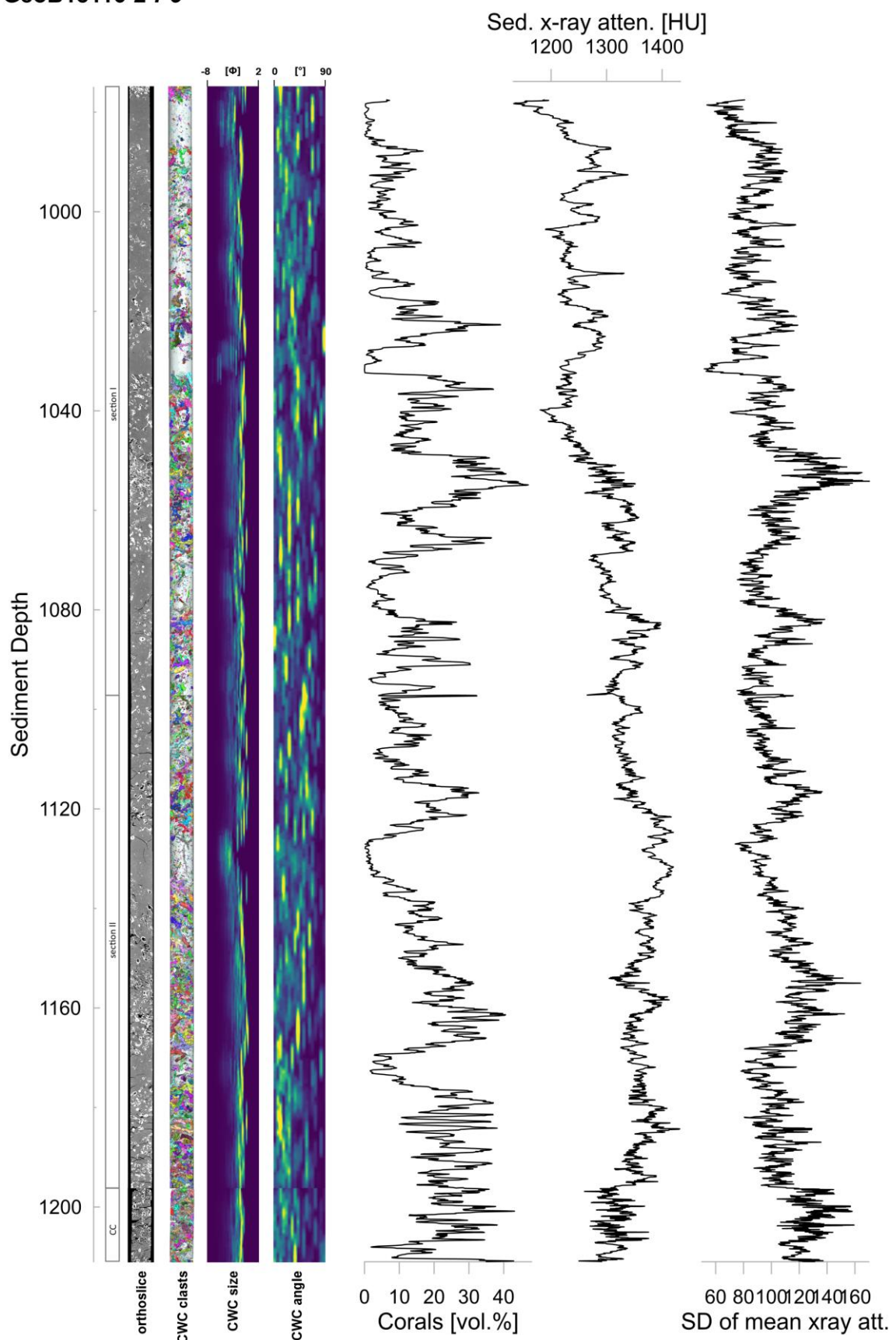


Fig. S13: CT-derived core data for GeoB18116-2 Barrel P5, with Sediment Depth as CSF-A (mbsf), orthoslice, section number (CC = core catcher), cold-water coral fossil clast quantification, size and angle, coral volume and mean x-ray attenuation in HU (Hounsfield units), and SD.

GeoB18116-2 P6

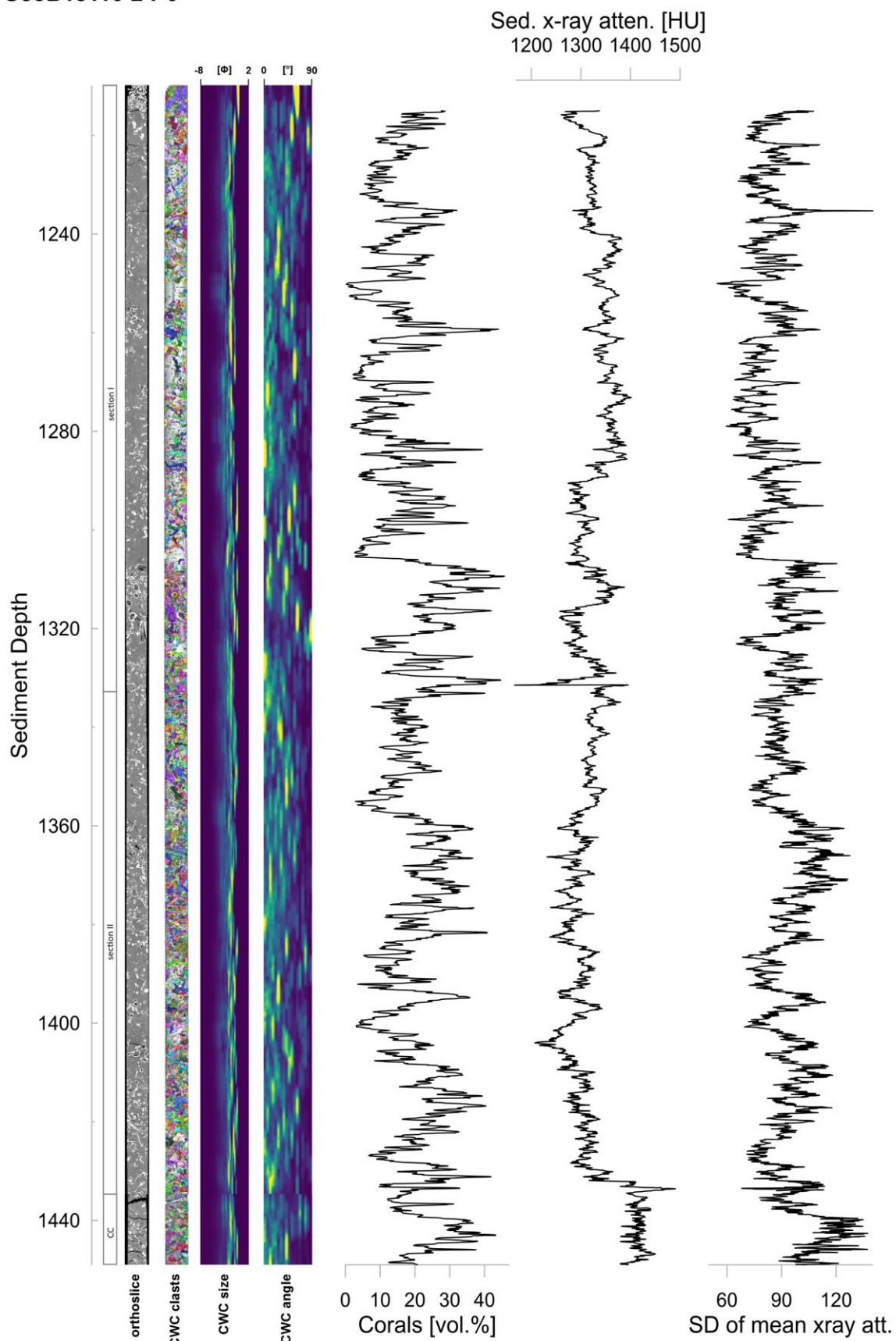


Fig. S14: CT-derived core data for GeoB18116-2 Barrel P6, with Sediment Depth as CSF-A (mbsf), orthoslice, section number (CC = core catcher), cold-water coral fossil clast quantification, size and angle, coral volume and mean x-ray attenuation in HU (Hounsfield units), and SD.

GeoB18116-2 P7

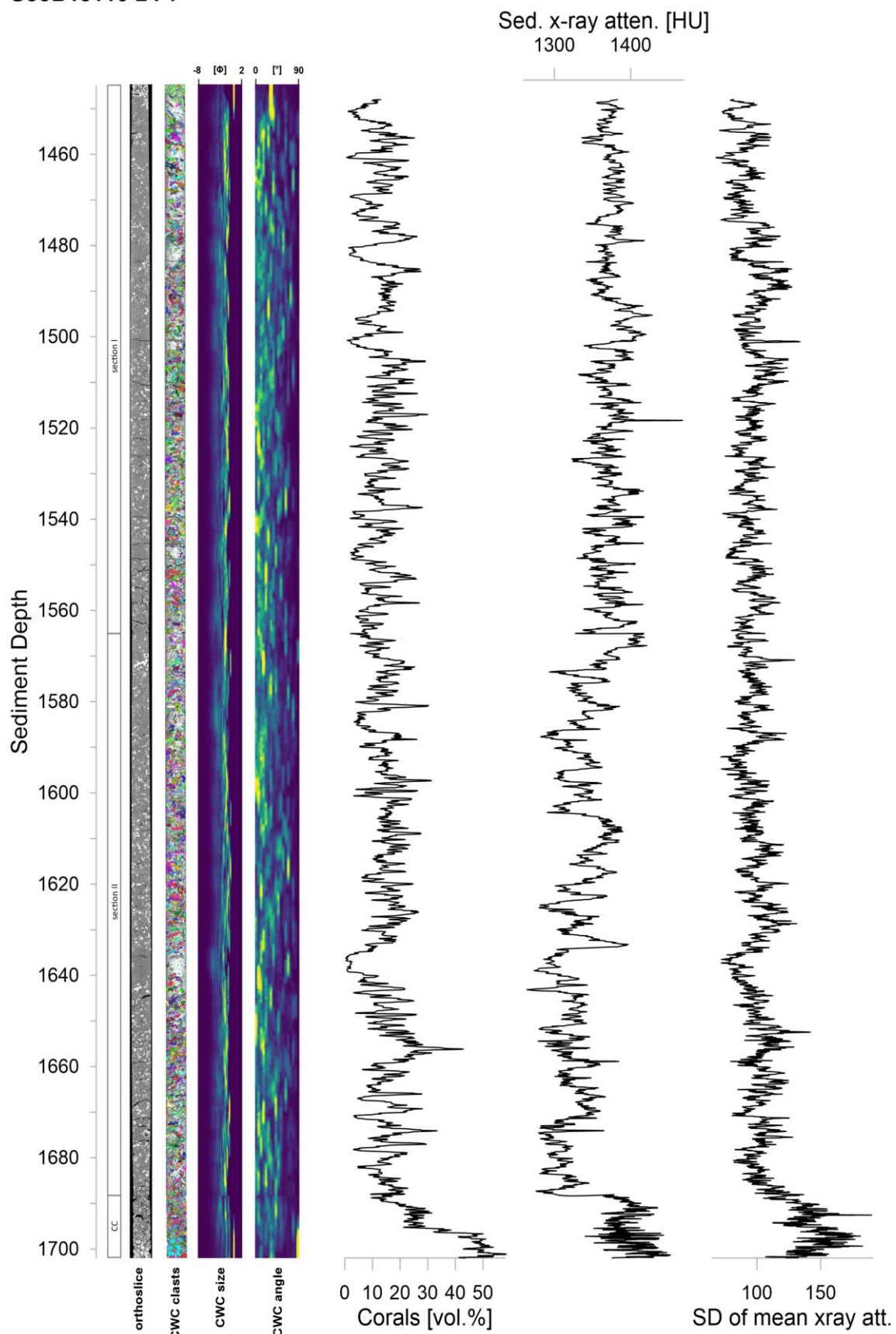


Fig. S15: CT-derived core data for GeoB18116-2 Barrel P7, with Sediment Depth as CSF-A (mbsf), orthoslice, section number (CC = core catcher), cold-water coral fossil clast quantification, size and angle, coral volume and mean x-ray attenuation in HU (Hounsfield units), and SD.

GeoB18116-2 P8

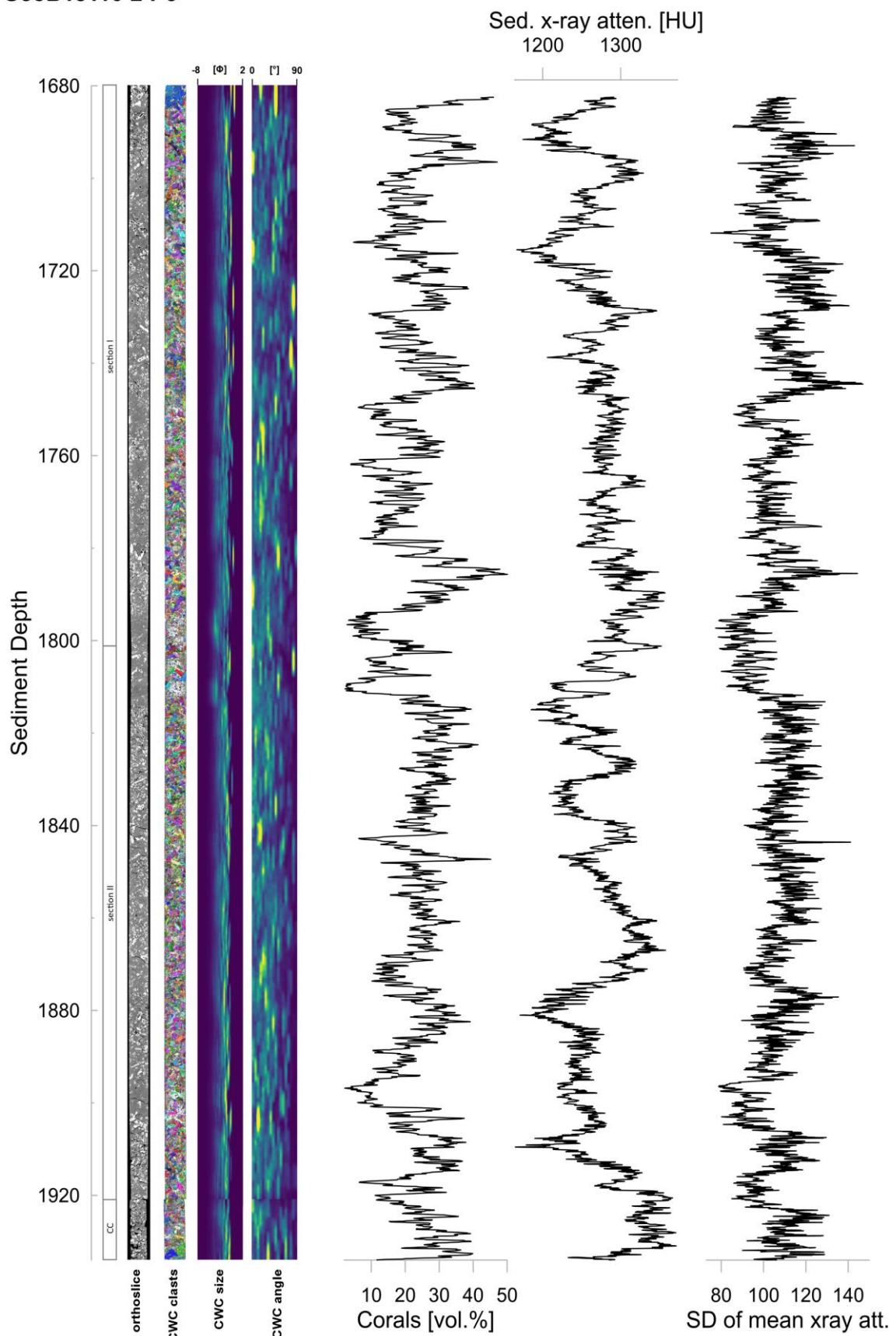


Fig. S16: CT-derived core data for GeoB18116-2 Barrel P8, with Sediment Depth as CSF-A (mbsf), orthoslice, section number (CC = core catcher), cold-water coral fossil clast quantification, size and angle, coral volume and mean x-ray attenuation in HU (Hounsfield units), and SD.

GeoB18116-2 P9

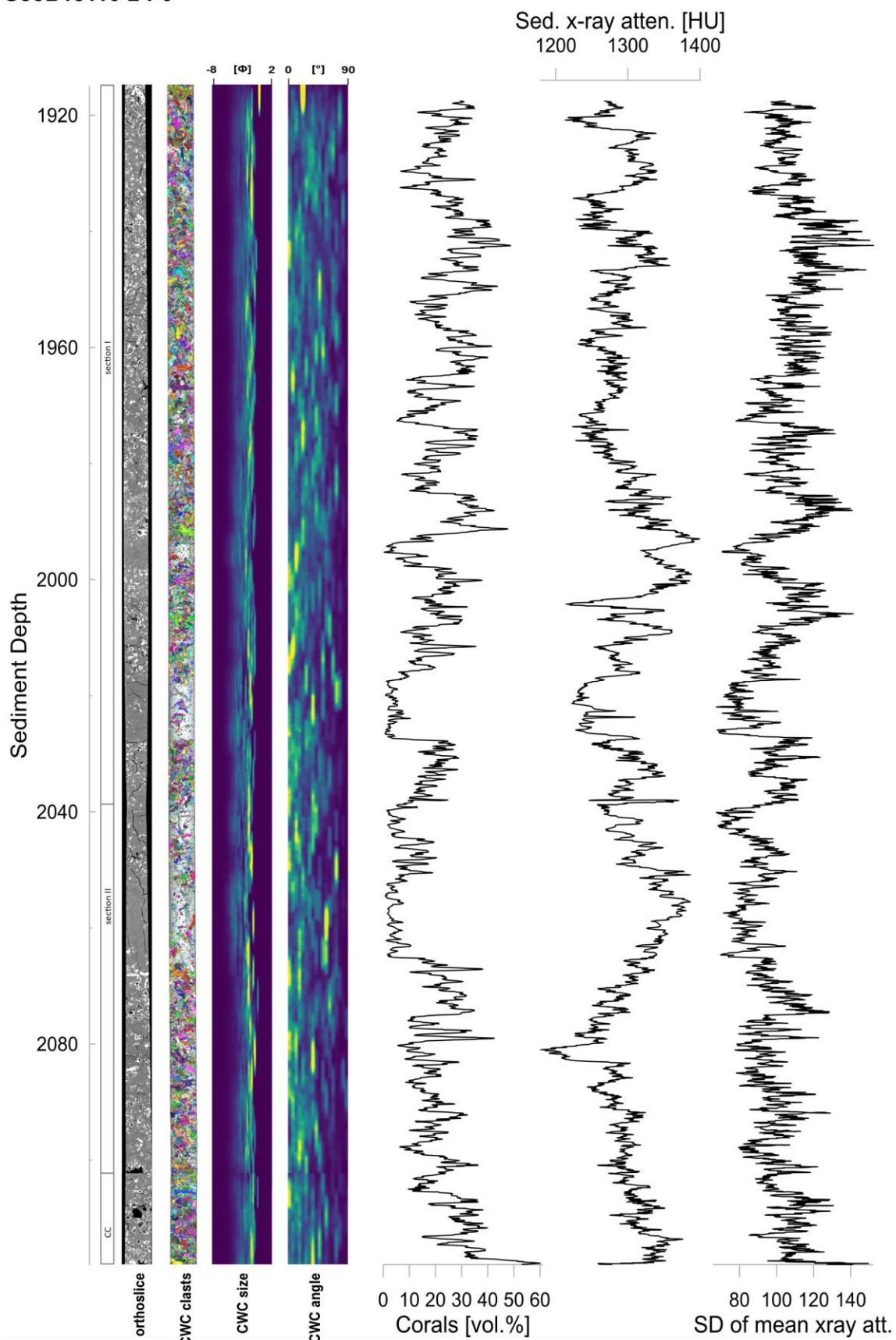


Fig. 17: CT-derived core data for GeoB18116-2 Barrel P9, with Sediment Depth as CSF-A (mbsf), orthoslice, section number (CC = core catcher), cold-water coral fossil clast quantification, size and angle, coral volume and mean x-ray attenuation in HU (Hounsfield units), and SD.

GeoB18116-2 P10

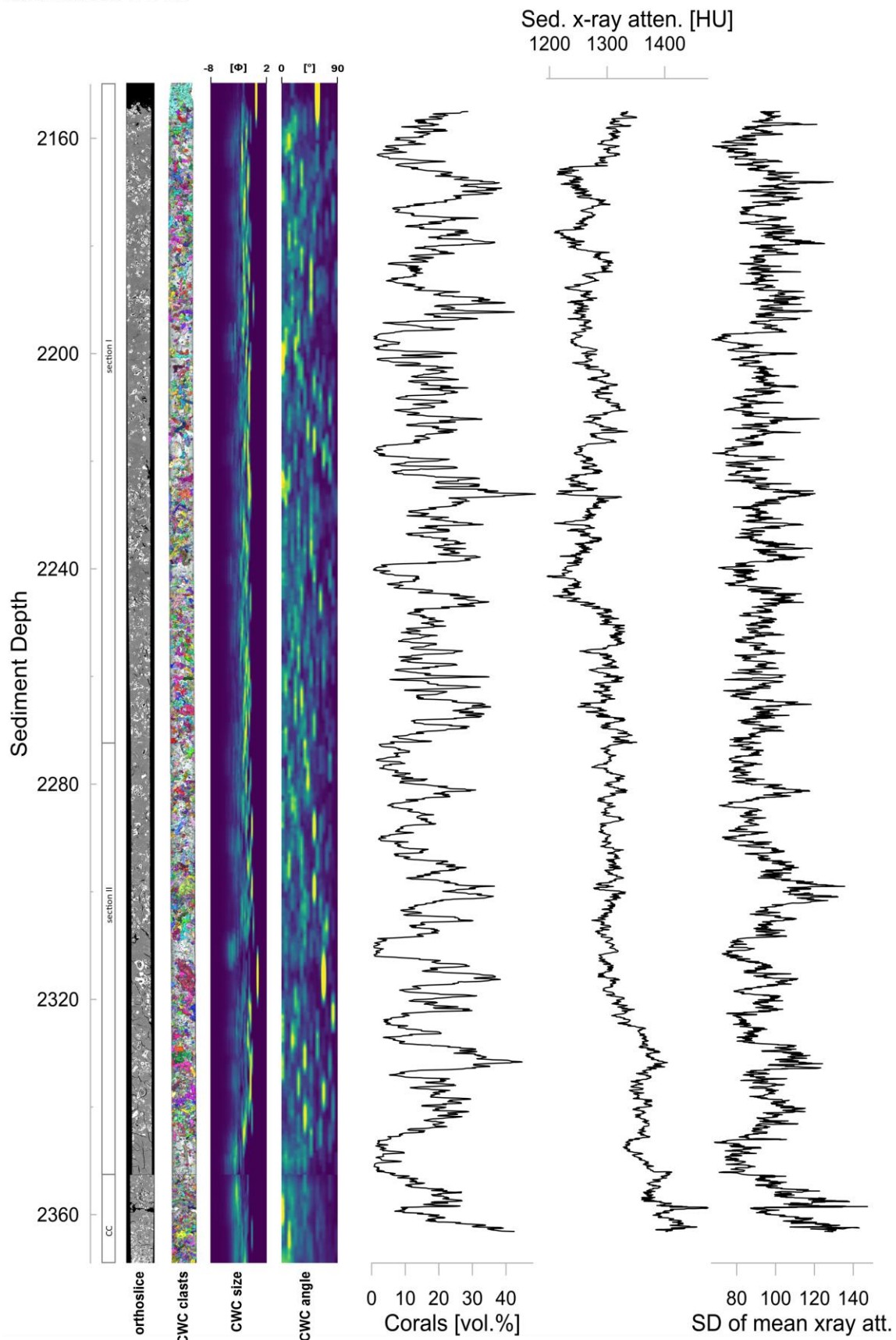


Fig. S18: CT-derived core data for GeoB18116-2 Barrel P10, with Sediment Depth as CSF-A (mbsf), orthoslice, section number (CC = core catcher), cold-water coral fossil clast quantification, size and angle, coral volume and mean x-ray attenuation in HU (Hounsfield units), and SD.

GeoB18116-2 P11

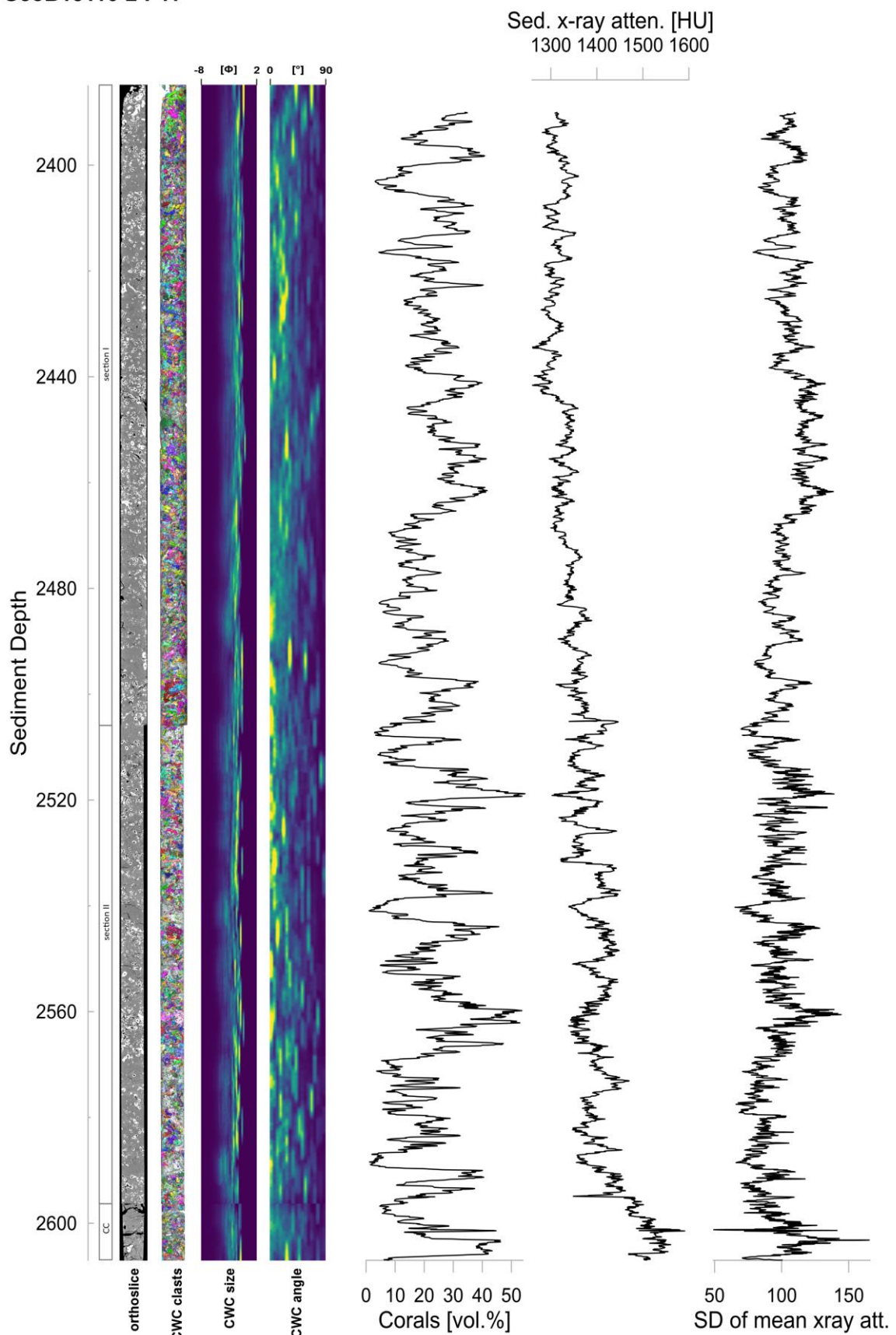


Fig. S19: CT-derived core data for GeoB18116-2 Barrel P11, with Sediment Depth as CSF-A (mbsf), orthoslice, section number (CC = core catcher), cold-water coral fossil clast quantification, size and angle, coral volume and mean x-ray attenuation in HU (Hounsfield units), and SD.

GeoB18116-2 P12

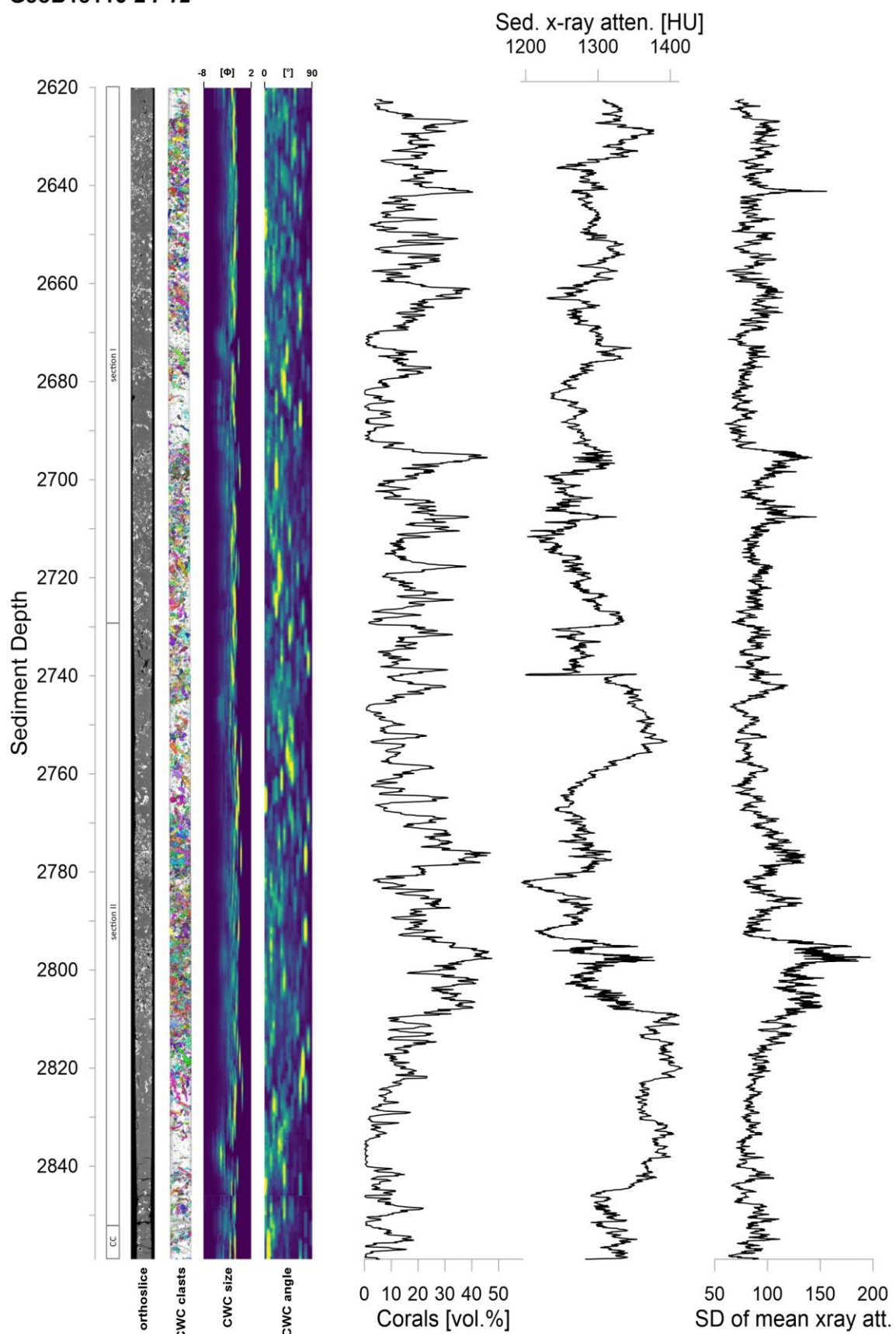


Fig. S20: CT-derived core data for GeoB18116-2 Barrel P12, with Sediment Depth as CSF-A (mbsf), orthoslice, section number (CC = core catcher), cold-water coral fossil clast quantification, size and angle, coral volume and mean x-ray attenuation in HU (Hounsfield units), and SD.

GeoB18116-2 P13

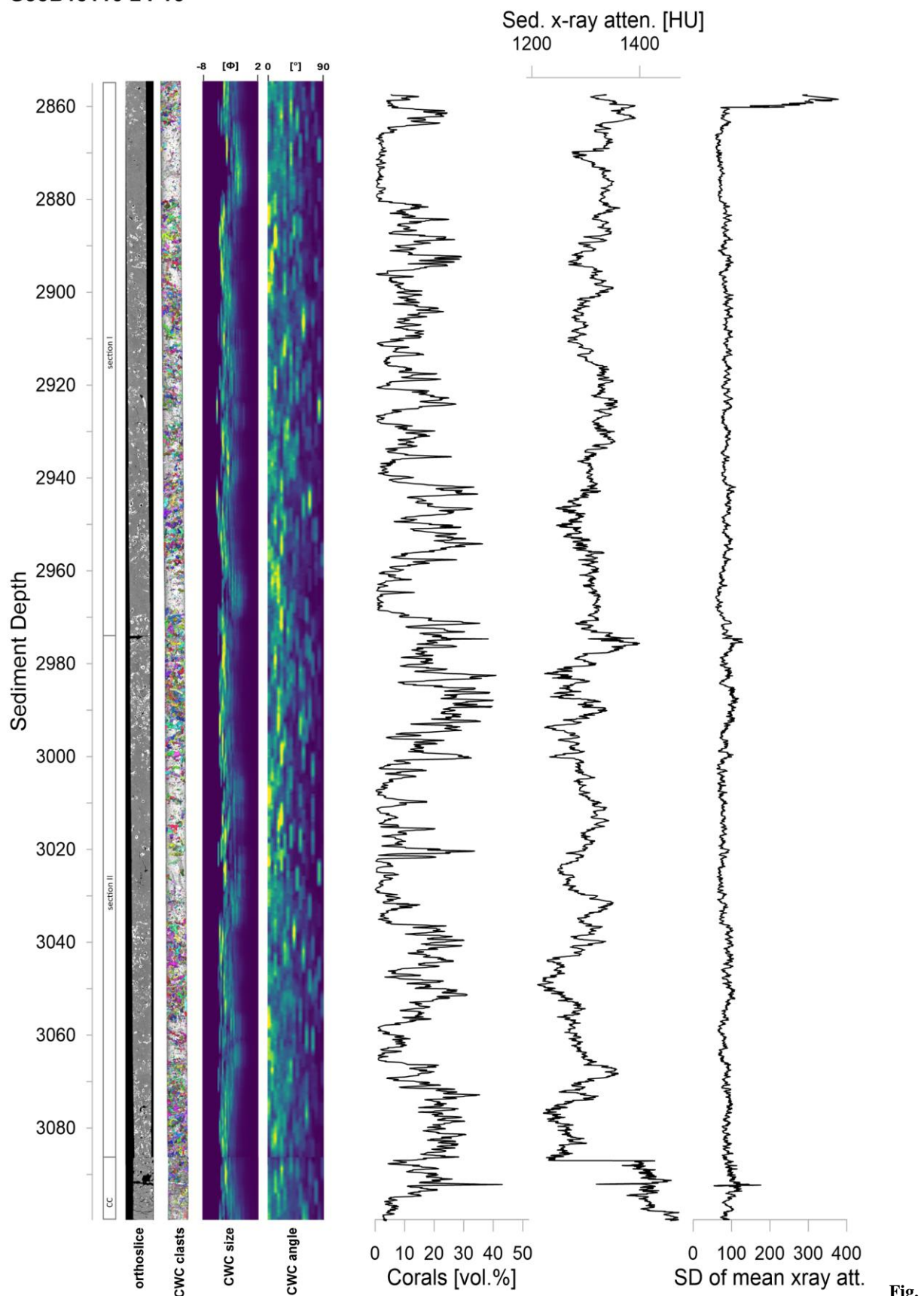


Fig.

S21: CT-derived core data for GeoB18116-2 Barrel P13, with Sediment Depth as CSF-A (mbsf), orthoslice, section number (CC = core catcher), cold-water coral fossil clast quantification, size and angle, coral volume and mean x-ray attenuation in HU (Hounsfield units), and SD.

GeoB18116-2 P14

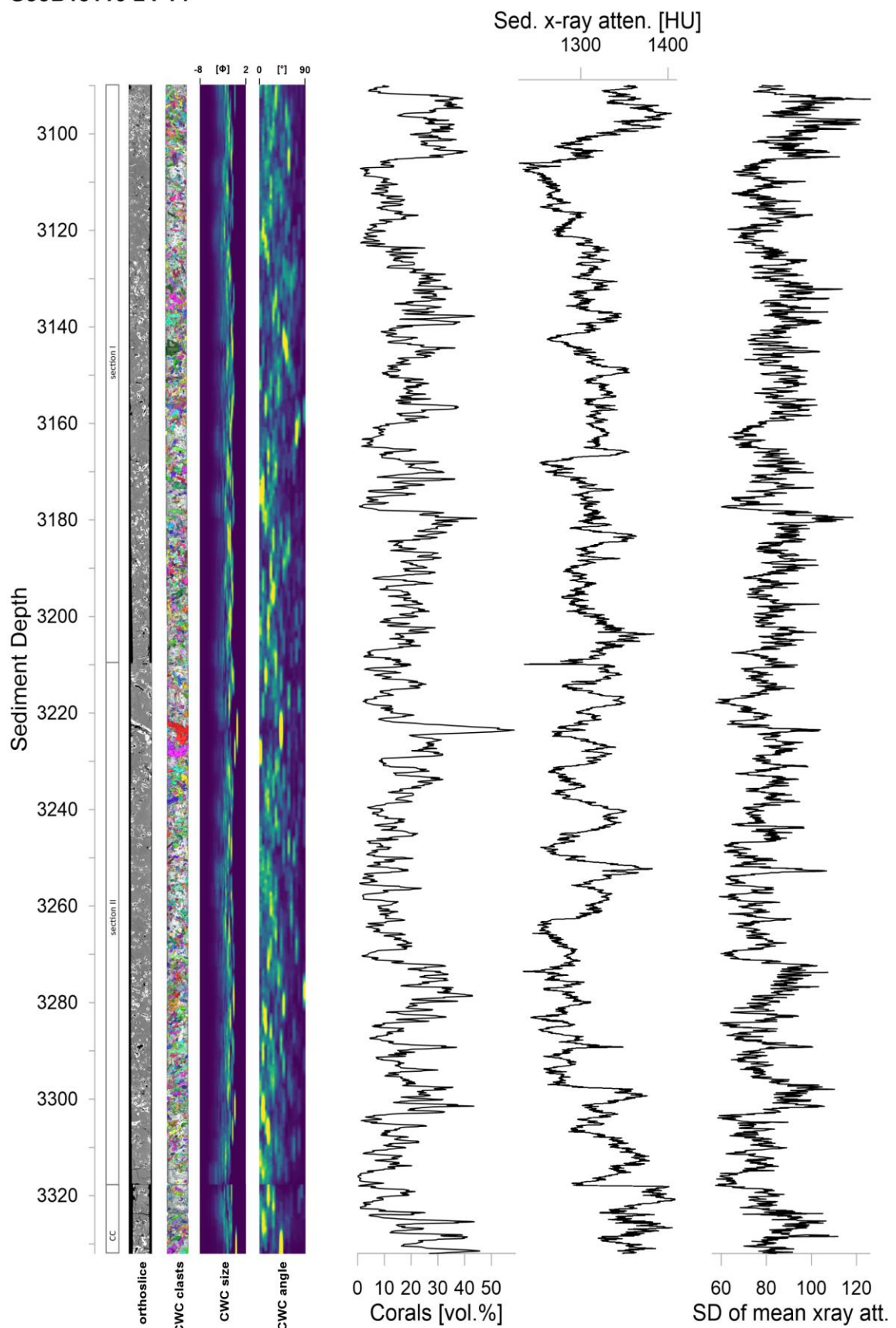


Fig. S22: CT-derived core data for GeoB18116-2 Barrel P14, with Sediment Depth as CSF-A (mbsf), orthoslice, section number (CC = core catcher), cold-water coral fossil clast quantification, size and angle, coral volume and mean x-ray attenuation in HU (Hounsfield units), and SD.

GeoB18116-2 P15

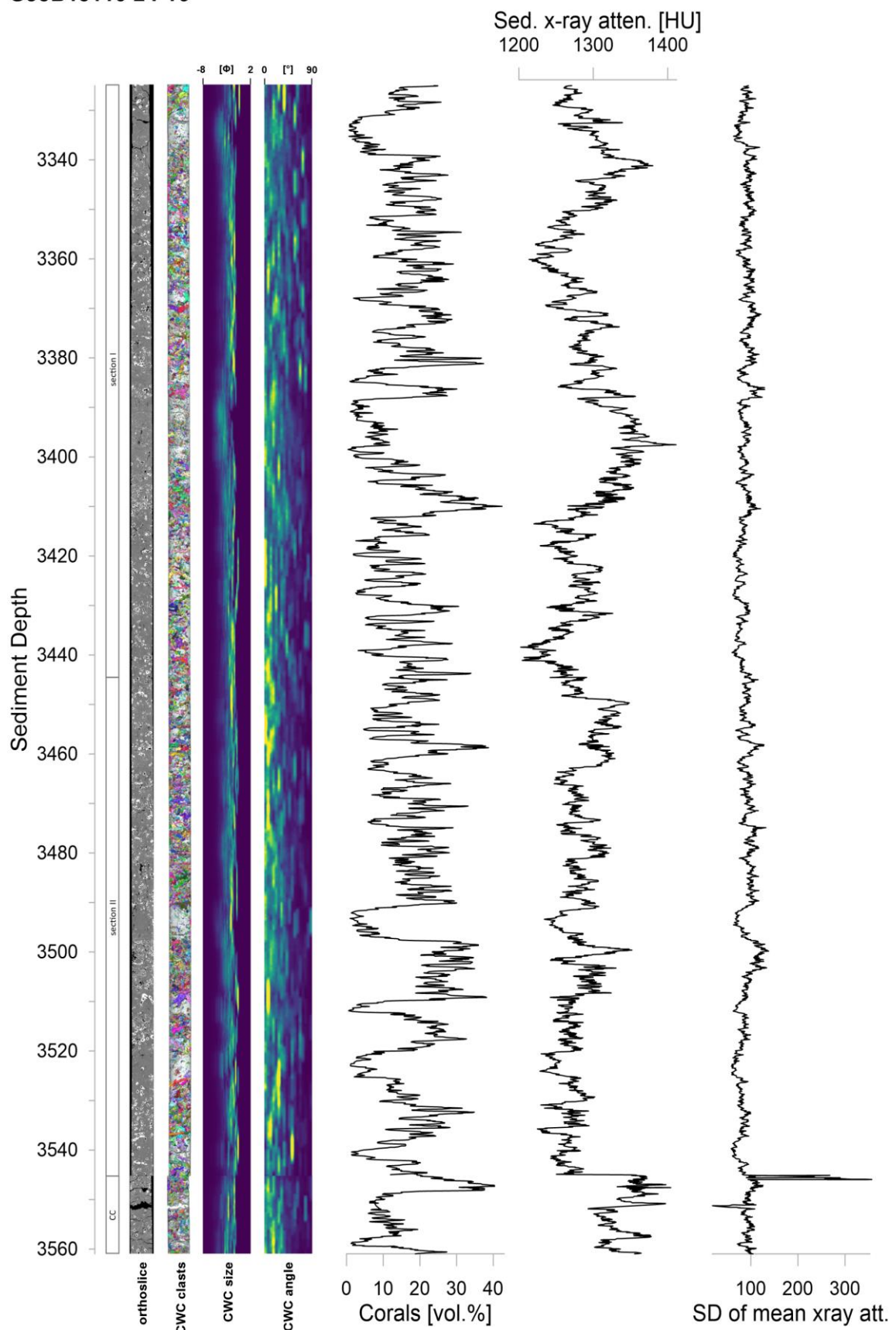


Fig. S23: CT-derived core data for GeoB18116-2 Barrel P15, with Sediment Depth as CSF-A (mbsf), orthoslice, section number (CC = core catcher), cold-water coral fossil clast quantification, size and angle, coral volume and mean x-ray attenuation in HU (Hounsfield units), and SD.

GeoB18116-2 P16

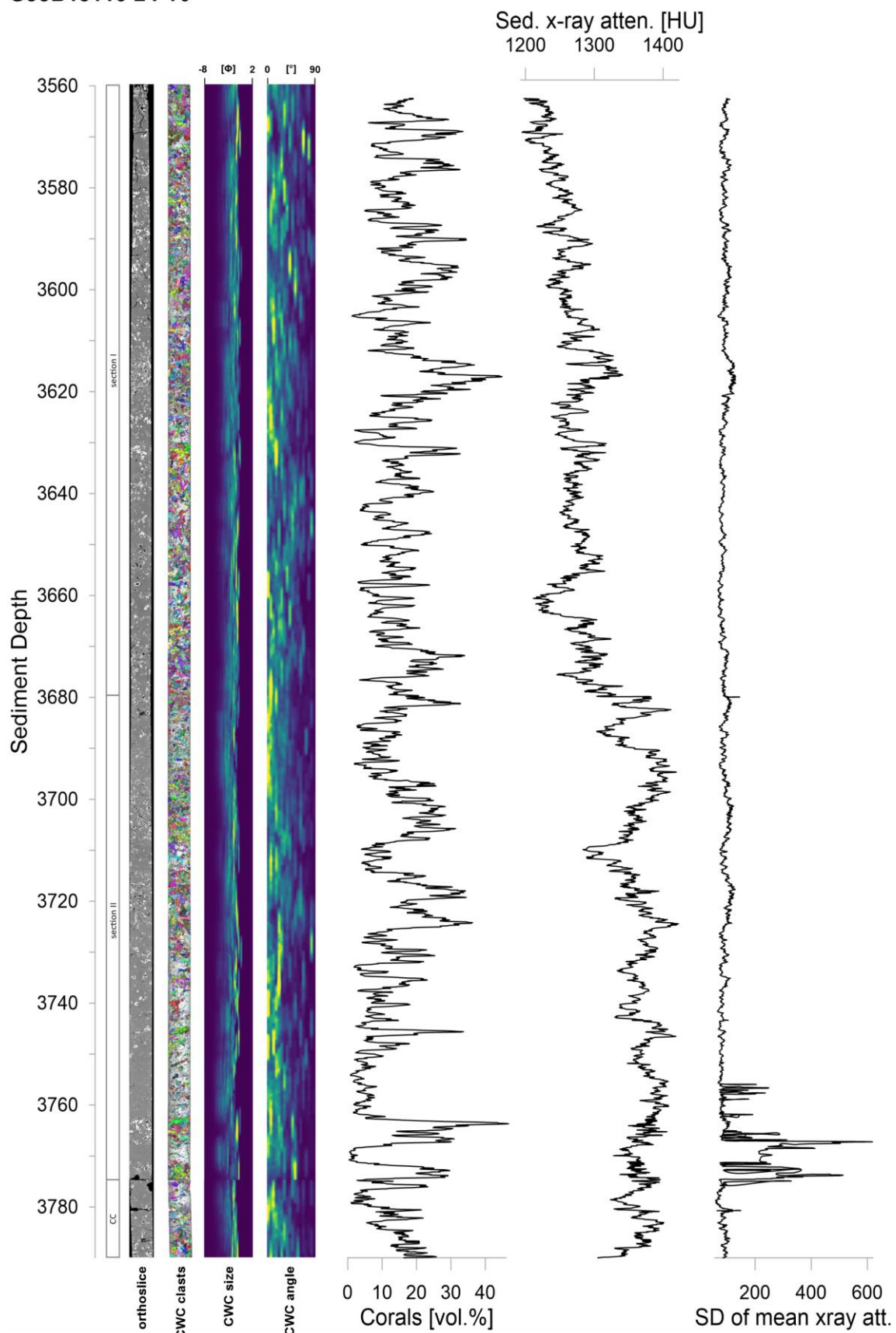


Fig. S24: CT-derived core data for GeoB18116-2 Barrel P16, with Sediment Depth as CSF-A (mbsf), orthoslice, section number (CC = core catcher), cold-water coral fossil clast quantification, size and angle, coral volume and mean x-ray attenuation in HU (Hounsfield units), and SD.

GeoB18116-2 P17

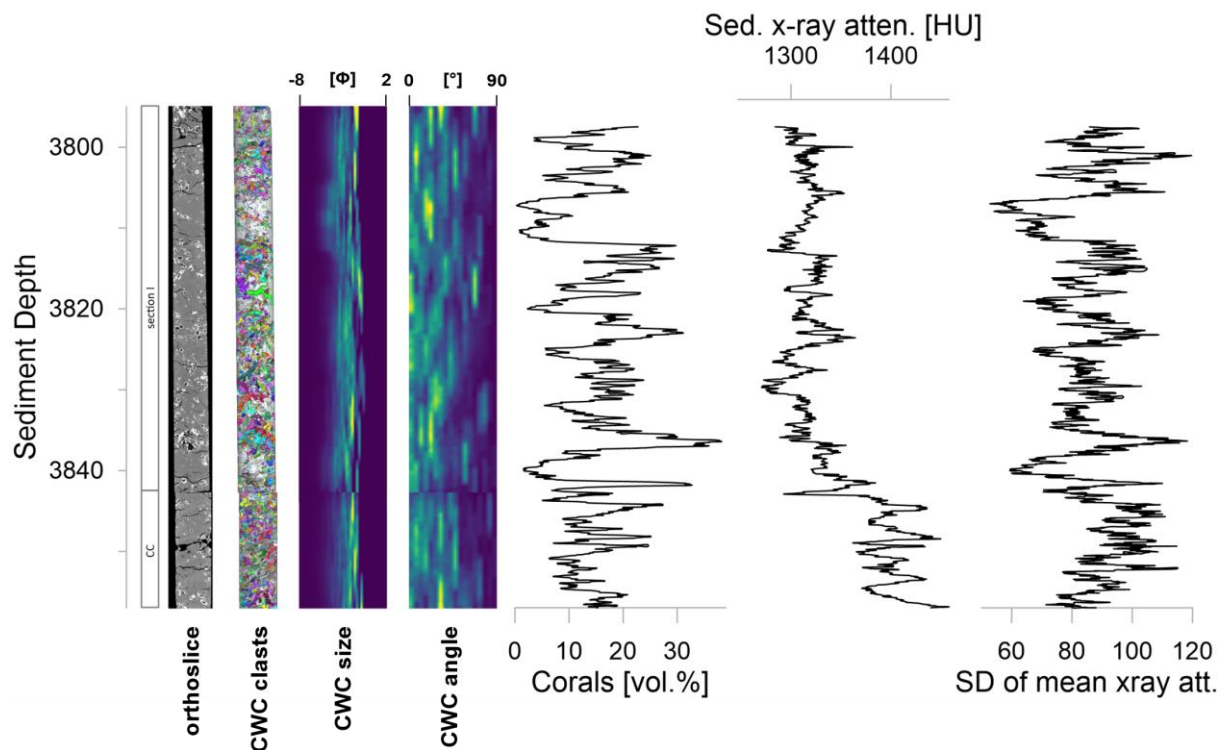


Fig. S25: CT-derived core data for GeoB18116-2 Barrel P17, with Sediment Depth as CSF-A (mbsf), orthoslice, section number (CC = core catcher), cold-water coral fossil clast quantification, size and angle, coral volume and mean x-ray attenuation in HU (Hounsfield units), and SD.

GeoB18116-2 P18

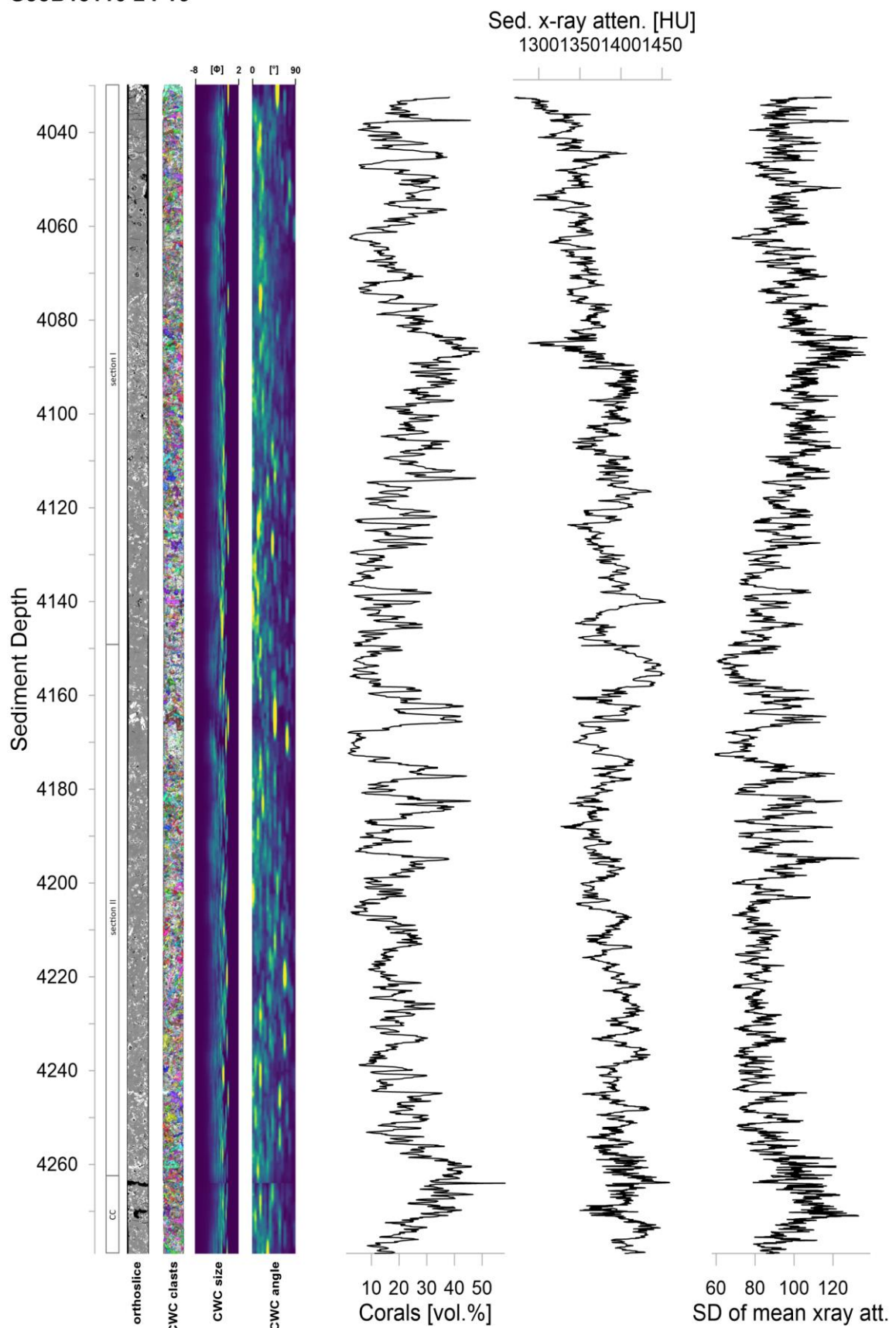


Fig. S26: CT-derived core data for GeoB18116-2 Barrel P18, with Sediment Depth as CSF-A (mbsf), orthoslice, section number (CC = core catcher), cold-water coral fossil clast quantification, size and angle, coral volume and mean x-ray attenuation in HU (Hounsfield units), and SD.

GeoB18116-2 P19

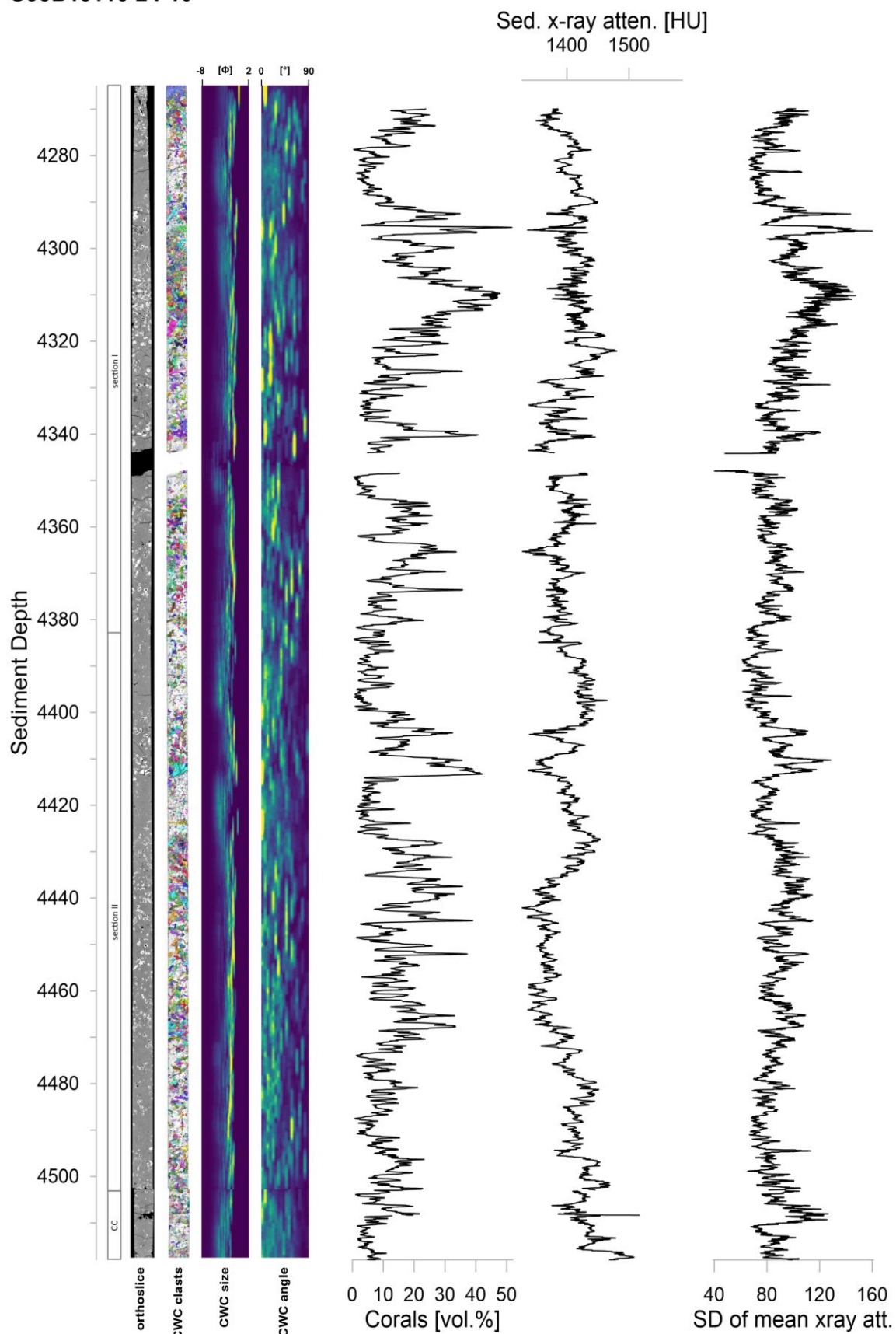


Fig. S27: CT-derived core data for GeoB18116-2 Barrel P19, with Sediment Depth as CSF-A (mbsf), orthoslice, section number (CC = core catcher), cold-water coral fossil clast quantification, size and angle, coral volume and mean x-ray attenuation in HU (Hounsfield units), and SD.

GeoB18116-2 P20

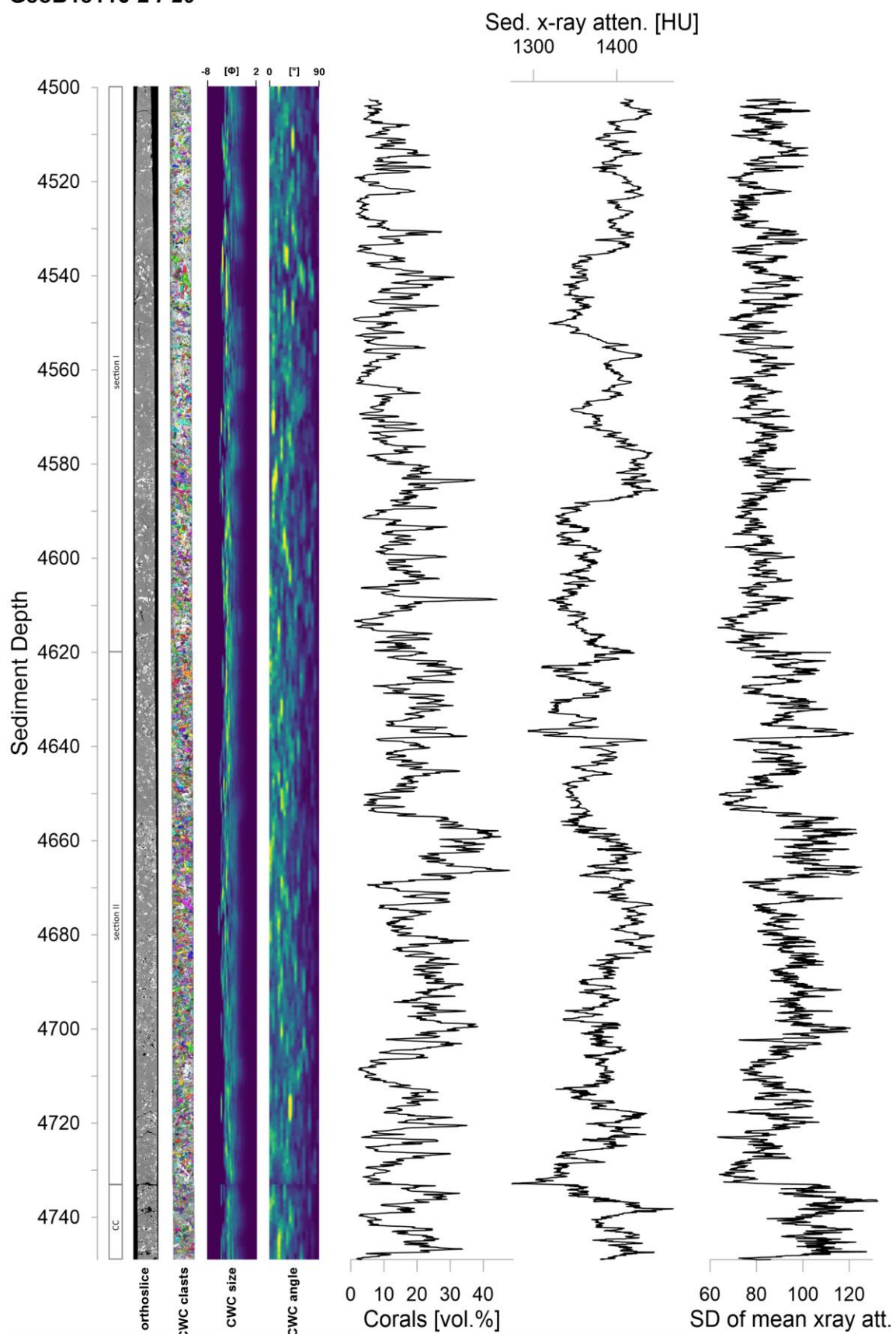


Fig. S28: CT-derived core data for GeoB18116-2 Barrel P20, with Sediment Depth as CSF-A (mbsf), orthoslice, section number (CC = core catcher), cold-water coral fossil clast quantification, size and angle, coral volume and mean x-ray attenuation in HU (Hounsfield units), and SD.

GeoB18116-2 P21

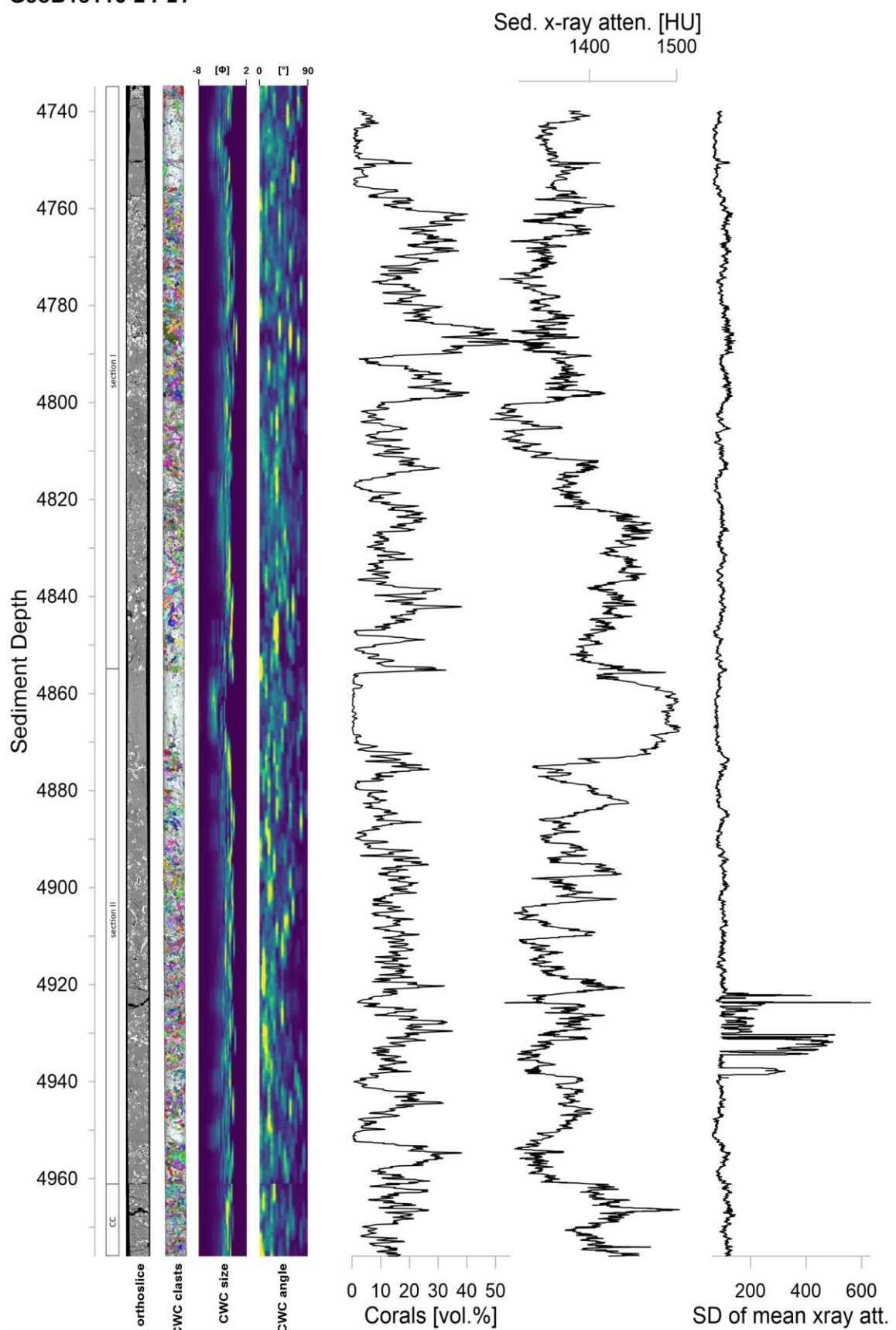


Fig. S29: CT-derived core data for GeoB18116-2 Barrel P21, with Sediment Depth as CSF-A (mbsf), orthoslice, section number (CC = core catcher), cold-water coral fossil clast quantification, size and angle, coral volume and mean x-ray attenuation in HU (Hounsfield units), and SD.

GeoB18116-2 P22

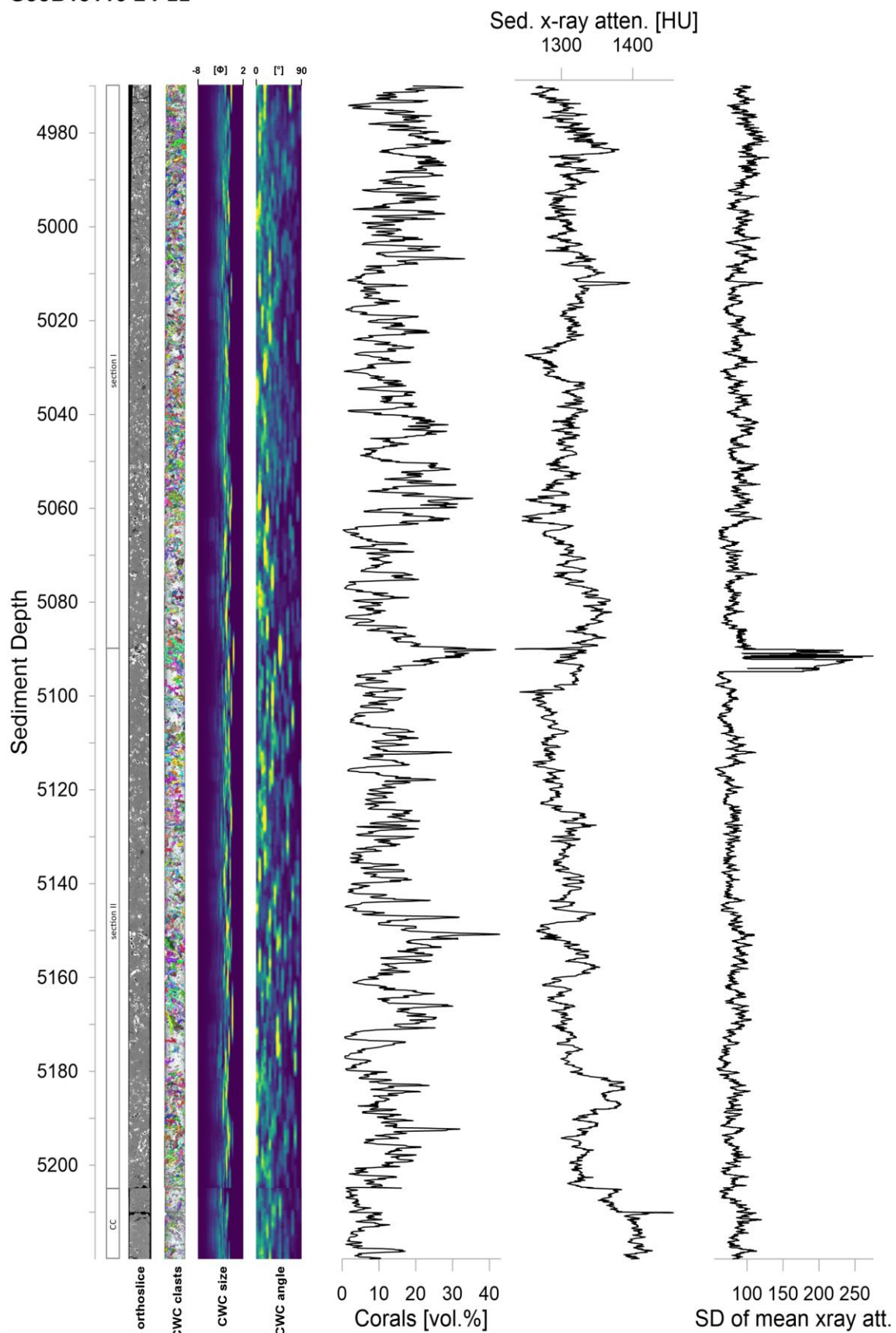


Fig. S30: CT-derived core data for GeoB18116-2 Barrel P22, with Sediment Depth as CSF-A (mbsf), orthoslice, section number (CC = core catcher), cold-water coral fossil clast quantification, size and angle, coral volume and mean x-ray attenuation in HU (Hounsfield units), and SD.

GeoB18116-2 P23

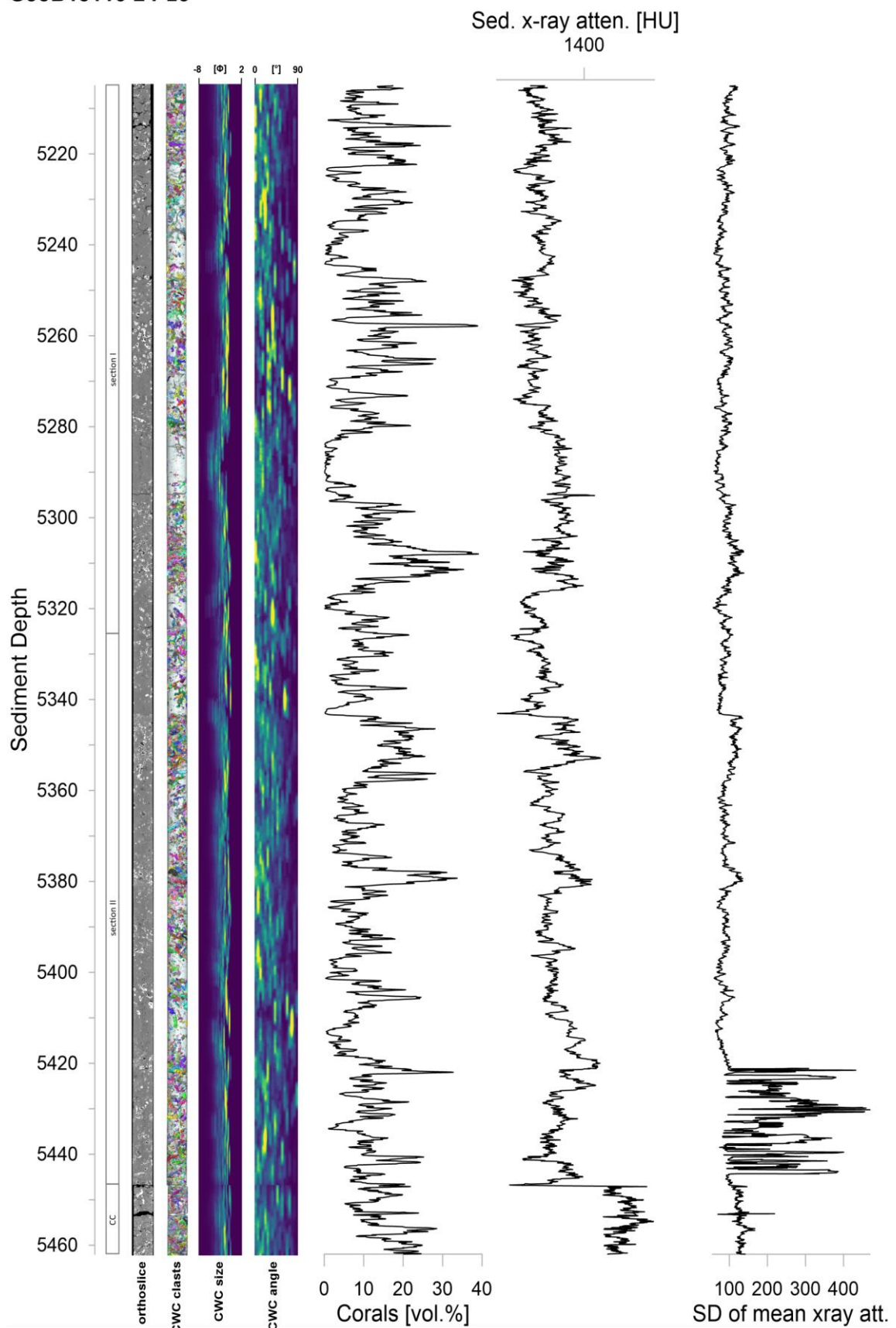


Fig. S31: CT-derived core data for GeoB18116-2 Barrel P23, with Sediment Depth as CSF-A (mbsf), orthoslice, section number (CC = core catcher), cold-water coral fossil clast quantification, size and angle, coral volume and mean x-ray attenuation in HU (Hounsfield units), and SD.

GeoB18116-2 P24

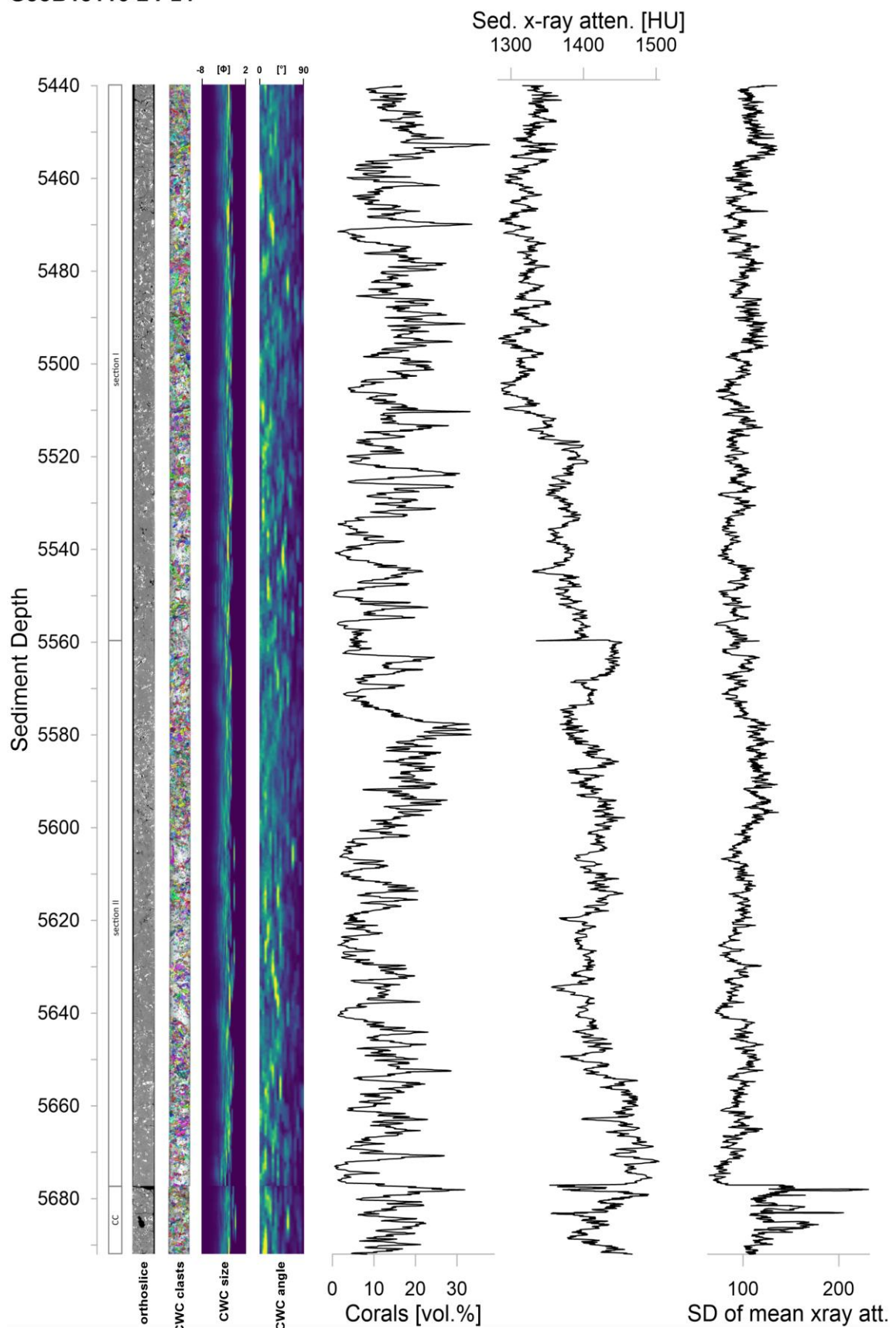


Fig. S32: CT-derived core data for GeoB18116-2 Barrel P24, with Sediment Depth as CSF-A (mbsf), orthoslice, section number (CC = core catcher), cold-water coral fossil clast quantification, size and angle, coral volume and mean x-ray attenuation in HU (Hounsfield units), and SD.

GeoB18116-2 P25

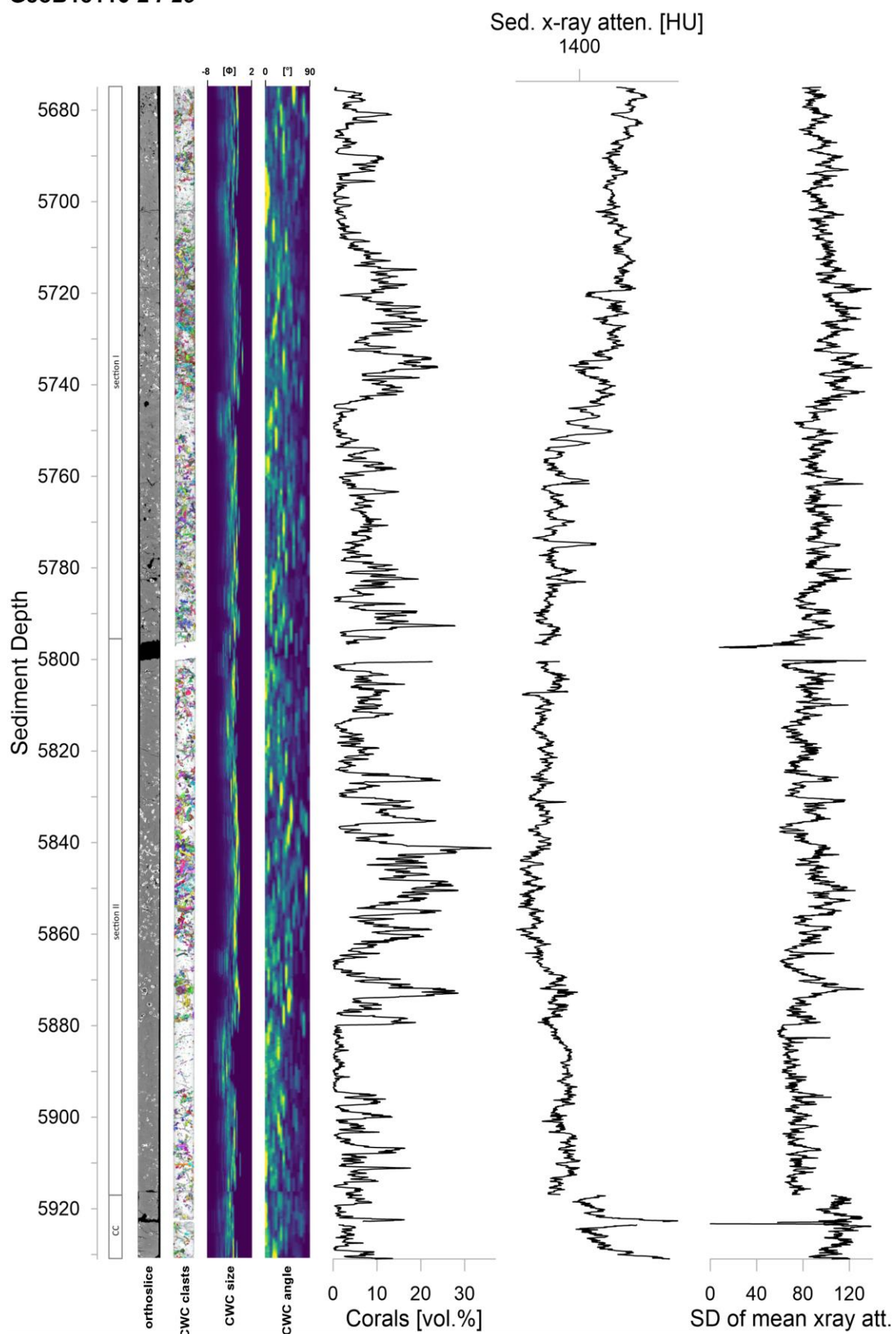


Fig. S33: CT-derived core data for GeoB18116-2 Barrel P25, with Sediment Depth as CSF-A (mbsf), orthoslice, section number (CC = core catcher), cold-water coral fossil clast quantification, size and angle, coral volume and mean x-ray attenuation in HU (Hounsfield units), and SD.

GeoB18116-2 P26

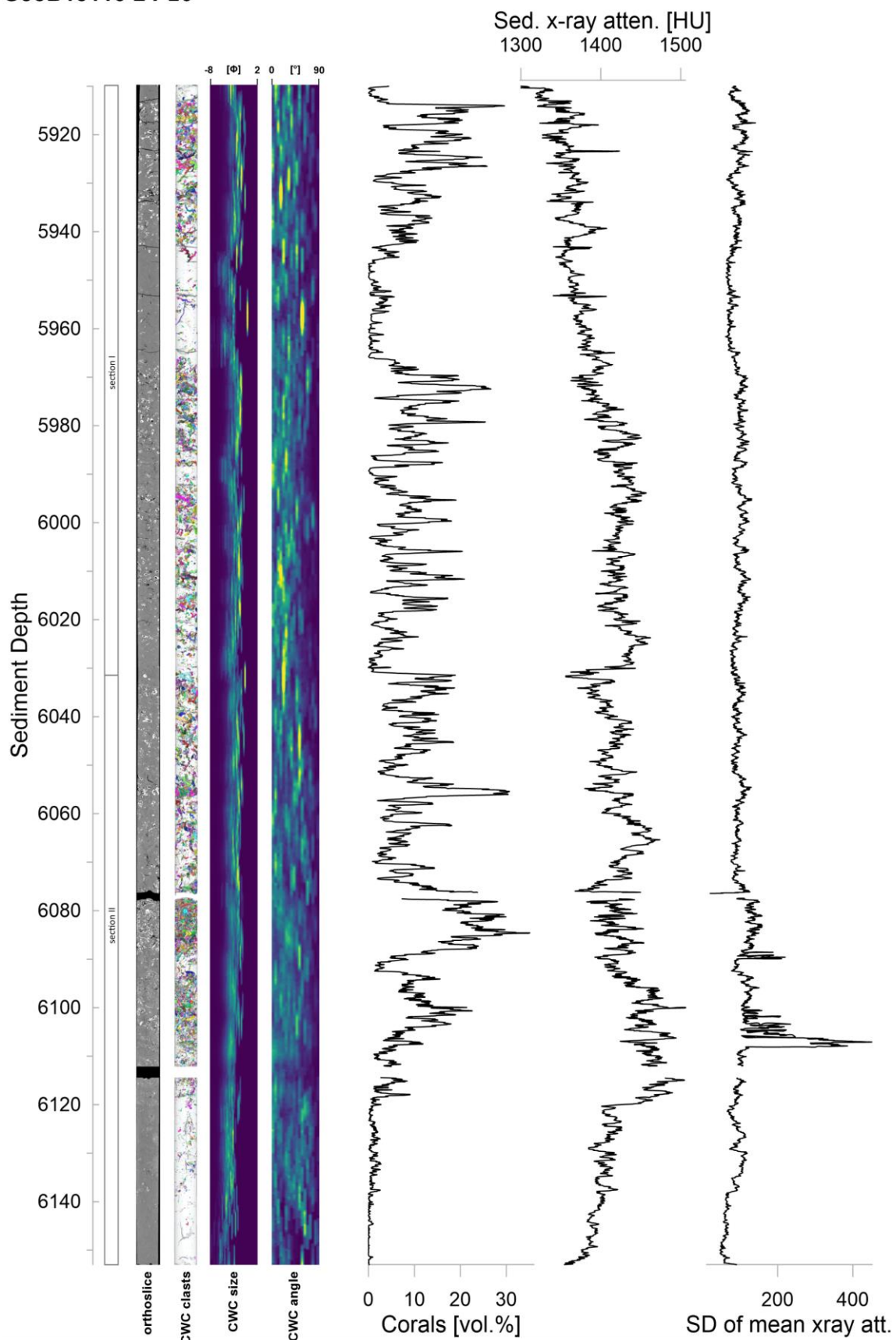


Fig. S34: CT-derived core data for GeoB18116-2 Barrel P26, with Sediment Depth as CSF-A (mbsf), orthoslice, section number (CC = core catcher), cold-water coral fossil clast quantification, size and angle, coral volume and mean x-ray attenuation in HU (Hounsfield units), and SD.